
Learning to Synthesize Programs as Interpretable and Generalizable Policies

Dweep Trivedi^{*†} Jesse Zhang^{*1} Shao-Hua Sun¹ Joseph J. Lim^{‡1}
¹University of Southern California
{dtrivedi, jessez, shaohuas, limjj}@usc.edu

Abstract

Recently, deep reinforcement learning (DRL) methods have achieved impressive performance on tasks in a variety of domains. However, neural network policies produced with DRL methods are not human-interpretable and often have difficulty generalizing to novel scenarios. To address these issues, prior works explore learning programmatic policies that are more interpretable and structured for generalization. Yet, these works either employ limited policy representations (e.g. decision trees, state machines, or predefined program templates) or require stronger supervision (e.g. input/output state pairs or expert demonstrations). We present a framework that instead learns to synthesize a program, which details the procedure to solve a task in a flexible and expressive manner, solely from reward signals. To alleviate the difficulty of learning to compose programs to induce the desired agent behavior from scratch, we propose to first learn a program embedding space that continuously parameterizes diverse behaviors in an unsupervised manner and then search over the learned program embedding space to yield a program that maximizes the return for a given task. Experimental results demonstrate that the proposed framework not only learns to reliably synthesize task-solving programs but also outperforms DRL and program synthesis baselines while producing interpretable and more generalizable policies. We also justify the necessity of the proposed two-stage learning scheme as well as analyze various methods for learning the program embedding. Website at <https://clvrai.com/leaps>.

1 Introduction

Recently, deep reinforcement learning (DRL) methods have demonstrated encouraging performance on a variety of domains such as outperforming humans in complex games [1–4] or controlling robots [5–11]. Despite the recent progress in the field, acquiring complex skills through trial and error still remains challenging and these neural network policies often have difficulty generalizing to novel scenarios. Moreover, such policies are not interpretable to humans and therefore are difficult to debug when these challenges arise.

To address these issues, a growing body of work aims to learn programmatic policies that are structured in more interpretable and generalizable representations such as decision trees [12], state-machines [13], and programs described by domain-specific programming languages [14, 15]. Yet, the programmatic representations employed in these works are often limited in expressiveness due to constraints on the policy spaces. For example, decision tree policies are incapable of naively generating repetitive behaviors, state machine policies used in [13] are computationally complex to

^{*}Contributed equally.

[†]Work partially done as a visiting scholar at USC.

[‡]AI Advisor at NAVER AI Lab.

scale to policies representing diverse behaviors, and the programs of [14, 15] are constrained to a set of predefined program templates. On the other hand, program synthesis works that aim to represent desired behaviors using flexible domain-specific programs often require extra supervision such as input/output pairs [16–20] or expert demonstrations [21, 22], which can be difficult to obtain.

In this paper, we present a framework to instead synthesize human-readable programs in an expressive representation, solely from rewards, to solve tasks described by Markov Decision Processes (MDPs). Specifically, we represent a policy using a program composed of control flows (*e.g.* if/else and loops) and an agent’s perceptions and actions. Our programs can flexibly compose behaviors through perception-conditioned loops and nested conditional statements. However, composing individual program tokens (*e.g.* if, while, move ()) in a trial-and-error fashion to synthesize programs that can solve given MDPs can be extremely difficult and inefficient.

To address this problem, we propose to first learn a latent program embedding space where nearby latent programs correspond to similar behaviors and allows for smooth interpolation, together with a program decoder that can decode a latent program to a program consisting of a sequence of program tokens. Then, when a task is given, this embedding space allows us to iteratively search over candidate latent programs to find a program that induces desired behavior to maximize the reward. Specifically, this embedding space is learned through reconstruction of randomly generated programs and the behaviors they induce in the environment in an unsupervised manner. Once learned, the embedding space can be reused to solve different tasks without retraining.

To evaluate the proposed framework, we consider the Karel domain [23], featuring an agent navigating through a gridworld and interacting with objects to solve tasks such as stacking and navigation. The experimental results demonstrate that the proposed framework not only learns to reliably synthesize task-solving programs but also outperforms program synthesis and deep RL baselines. In addition, we justify the necessity of the proposed two-stage learning scheme as well as conduct an extensive analysis comparing various approaches for learning the latent program embedding spaces. Finally, we perform experiments which highlight that the programs produced by our proposed framework can both generalize to larger state spaces and unseen state configurations as well as be interpreted and edited by humans to improve their task performance.

2 Related Work

Neural program induction and synthesis. Program induction methods [20, 24–36] aim to implicitly induce the underlying programs to mimic the behaviors demonstrated in given task specifications such as input/output pairs or expert demonstrations. On the other hand, program synthesis methods [16–19, 21, 37–58] explicitly synthesize the underlying programs and execute the programs to perform the tasks from task specifications such input/output pairs, demonstrations, language instructions. In contrast, we aim to learn to synthesize programs solely from reward described by an MDP without other task specifications. Similarly to us, a two-stage synthesis method is proposed in [46]. Yet, the task is to match truth tables for given test programs rather than solve MDPs. Their first stage requires the entire ground-truth table for each program synthesized during training, which is infeasible to apply to our problem setup (*i.e.* synthesizing imperative programs for solving MDPs).

Learning programmatic policies. Prior works have also addressed the problem of learning programmatic policies [59–61]. Bastani et al. [12] learns a decision tree as a programmatic policy for pong and cartpole environments by imitating an oracle neural policy. However, decision trees are incapable of representing repeating behaviors on their own. Silver et al. [49] addresses this by including a loop-style token for their decision tree policy, though it is still not as expressive as synthesized loops. Inala et al. [13] learns programmatic policies as finite state machines by imitating a teacher policy, although finite state machine complexity can scale quadratically with the number of states, making them difficult to scale to more complex behaviors.

Another line of work instead synthesizes programs structured in Domain Specific Languages (DSLs), allowing humans to design tokens (*e.g.* conditions and operations) and control flows (*e.g.* while loops, if statements, reusable functions) to induce desired behaviors and can produce human interpretable programs. Verma et al. [14, 15] distill neural network policies into programmatic policies. Yet, the initial programs are constrained to a set of predefined program templates. This significantly limits the scope of synthesizable programs and requires designing such templates for each task. In contrast,

our method can synthesize diverse programs, without templates, which can flexibly represent the complex behaviors required to solve various tasks.

3 Problem Formulation

We are interested in learning to synthesize a program structured in a given DSL that can be executed to solve a given task described by an MDP, purely from reward. In this section, we formally define our definition of a program and DSL, tasks described by MDPs, and the problem formulation.

Program and Domain Specific Language. The programs, or programmatic policies, considered in this work are defined based on a DSL as shown in Figure 1. The DSL consists of control flows and an agent’s perceptions and actions. A perception indicates circumstances in the environment (*e.g.* `frontIsClear()`) that can be perceived by an agent, while an action defines a certain behavior that can be performed by an agent (*e.g.* `move()`, `turnLeft()`). Control flow includes `if/else` statements, loops, and boolean/logical operators to compose more sophisticated conditions. A policy considered in this work is described by a program ρ which is executed to produce a sequence of actions given perceptions from the environment.

Program ρ :=	DEF run m(s m)
Repetition n :=	Number of repetitions
Perception h :=	Domain-dependent perceptions
Condition b :=	perception h not perception h
Action a :=	Domain-dependent actions
Statement s :=	while c(b c) w(s w) s ₁ ; s ₂ a repeat R=n r(s r) if c(b c) i(s i) ifelse c(b c) i(s ₁ i) else e(s ₂ e)

Figure 1: The domain-specific language (DSL) for constructing programs.

MDP. We consider finite-horizon discounted MDPs with initial state distribution $\mu(s_0)$ and discount factor γ . For a fixed sequence $\{(s_0, a_0), \dots, (s_t, a_t)\}$ of states and actions obtained from a rollout of a given policy, the performance of the policy is evaluated based on a discounted return $\sum_{t=0}^T \gamma^t r_t$, where T is the horizon of the episode and $r_t = \mathcal{R}(s_t, a_t)$ the reward function.

Objective. Our objective is $\max_{\rho} \mathbb{E}_{a \sim \text{EXEC}(\rho), s_0 \sim \mu} [\sum_{t=0}^T \gamma^t r_t]$, where EXEC returns the actions induced by executing a program policy ρ in the environment. Note that one can view this objective as a special case of the standard RL objective, where the policy is represented as a program which follows the grammar of the DSL and the policy rollout is obtained by executing the program.

4 Approach

Our goal is to develop a framework that can synthesize a program (*i.e.* a programmatic policy) structured in a given DSL that can be executed to solve a task of interest. This requires the ability to synthesize a program that is not only valid for execution (*e.g.* grammatically correct) but also describes desired behaviors for solving the task from only the reward. Yet, learning to synthesize such a program from scratch for every new task can be difficult and inefficient.

To this end, we propose our Learning Embeddings for lAtent Program Synthesis framework, dubbed LEAPS, as illustrated in Figure 2. LEAPS first learns a latent program embedding space that continuously parameterizes diverse behaviors and a program decoder that decodes a latent program to a program consisting of a sequence of program tokens. Then, when a task is given, we iteratively search over this embedding space and decode each candidate latent program using the decoder to find a program that maximizes the reward. This two-stage learning scheme not only enables learning to synthesize programs to acquire desired behaviors described by MDPs solely from reward, but also allows reusing the learned embedding space to solve different tasks without retraining.

In the rest of this section, we describe how we construct the model and our learning objectives for the latent program embedding space in Section 4.1. Then, we present how a program that describes desired behaviors for a given task can be found through a search algorithm in Section 4.2.

4.1 Learning a Program Embedding Space

To learn a latent program embedding space, we propose to train a variational autoencoder (VAE) [62] that consists of a program encoder q_{ϕ} which encodes a program ρ to a latent program z and a program decoder p_{θ} which reconstructs the program from the latent. Specifically, the VAE is trained through

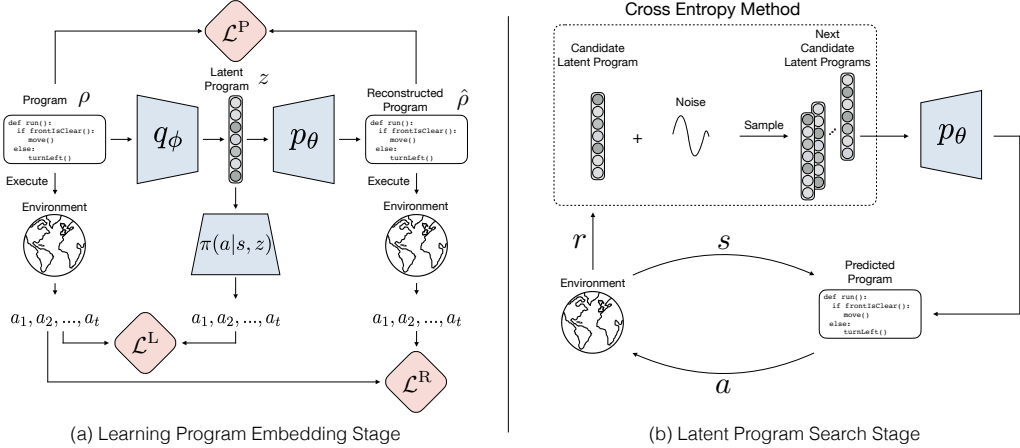


Figure 2: (a) **Learning program embedding stage**: we propose to learn a program embedding space by training a program encoder q_ϕ that encodes a program as a latent program z , a program decoder p_θ that decodes the latent program z back to a reconstructed program $\hat{\rho}$, and a policy π that conditions on the latent program z and acts as a neural program executor to produce the execution trace of the latent program z . The model optimizes a combination of a program reconstruction loss \mathcal{L}^P , a program behavior reconstruction loss \mathcal{L}^R , and a latent behavior reconstruction loss \mathcal{L}^L . a_1, a_2, \dots, a_t denotes actions produced by either the policy π or program execution. (b) **Latent program search stage**: we use the Cross Entropy Method to iteratively search for the best candidate latent programs that can be decoded and executed to maximize the reward to solve given tasks.

reconstruction of randomly generated programs and the behaviors they induce in the environment in an unsupervised manner. Architectural details are listed in Section L.6.

Since we aim to iteratively search over the learned embedding space to achieve certain behaviors when a task is given, we want this embedding space to allow for smooth behavior interpolation (*i.e.* programs that exhibit similar behaviors are encoded closer in the embedding space). To this end, we propose to train the model by optimizing the following three objectives.

4.1.1 Program Reconstruction

To learn a program embedding space, we train a program encoder q_ϕ and a program decoder p_θ to reconstruct programs composed of sequences of program tokens. Given an input program ρ consisting of a sequence of program tokens, the encoder processes the input program one token at a time and produces a latent program embedding z . Then, the decoder outputs program tokens one by one from the latent program embedding z to synthesize a reconstructed program $\hat{\rho}$. Both the encoder and the decoder are recurrent neural networks and are trained to optimize the β -VAE [63] loss:

$$\mathcal{L}_{\theta, \phi}^P(\rho) = -\mathbb{E}_{z \sim q_\phi(z|\rho)}[\log p_\theta(\rho|z)] + \beta D_{\text{KL}}(q_\phi(z|\rho) \| p_\theta(z)). \quad (1)$$

4.1.2 Program Behavior Reconstruction

While the loss in Eq. 1 enforces that the model encodes syntactically similar programs close to each other in the embedding space, we also want to encourage programs with the same semantics to have similar program embeddings. An example that demonstrates the importance of this is the *program aliasing* issue, where different programs have identical program semantics (*e.g.* `repeat(2): move()` and `move() move()`). Thus, we introduce an objective that compares the execution traces of the input program and the reconstructed program. Since the program execution process is not differentiable, we optimize the model via REINFORCE [64]:

$$\mathcal{L}_{\theta, \phi}^R(\rho) = -\mathbb{E}_{z \sim q_\phi(z|\rho)}[R_{\text{mat}}(p_\theta(\rho|z), \rho)], \quad (2)$$

where $R_{\text{mat}}(\hat{\rho}, \rho)$, the reward for matching the input program’s behavior, is defined as

$$R_{\text{mat}}(\hat{\rho}, \rho) = \mathbb{E}_{\mu} \left[\frac{1}{N} \sum_{t=1}^N \underbrace{\mathbb{1}\{\text{EXEC}_i(\hat{\rho}) == \text{EXEC}_i(\rho) \forall i = 1, 2, \dots, t\}}_{\text{stays 0 after the first } t \text{ where } \text{EXEC}_t(\hat{\rho}) \neq \text{EXEC}_t(\rho)} \right], \quad (3)$$

where N is the maximum of the lengths of the execution traces of both programs, and $\text{EXEC}_i(\rho)$ represents the action taken by program ρ at time i . Thus this objective encourages the model to embed behaviorally similar yet possibly syntactically different programs to similar latent programs.

4.1.3 Latent Behavior Reconstruction

To further encourage learning a program embedding space that allows for smooth behavior interpolation, we devise another source of supervision by learning a program embedding-conditioned policy. Denoted $\pi(a|z, s_t)$, this recurrent policy takes the program embedding z produced by the program encoder and learns to predict corresponding agent actions. One can view this policy as a neural program executor that allows gradient propagation through the policy and the program encoder by optimizing the cross entropy between the actions obtained by executing the input program ρ and the actions predicted by the policy:

$$\mathcal{L}_{\pi}^{\text{L}}(\rho, \pi) = -\mathbb{E}_{\mu} \left[\sum_{t=1}^M \sum_{i=1}^{|\mathcal{A}|} \mathbb{1}\{\text{EXEC}_i(\hat{\rho}) == \text{EXEC}_i(\rho)\} \log \pi(a_i|z, s_t) \right], \quad (4)$$

where M denotes the length of the execution of ρ . Optimizing this objective directly encourages the program embeddings, through supervised learning instead of RL as in \mathcal{L}^{R} , to be useful for action reconstruction, thus further ensuring that similar behaviors are encoded together and allowing for smooth interpolation. Note that this policy is only used for improving learning the program embedding space not for solving the tasks of interest in the later stage.

In summary, we propose to optimize three sources of supervision to learn the program embedding space that allows for smooth interpolation and can be used to search for desired agent behaviors: (1) \mathcal{L}^{P} (Eq. 1), the β -VAE objective for program reconstruction, (2) \mathcal{L}^{R} (Eq. 2), an RL environment-state matching loss for the reconstructed program, and (3) \mathcal{L}^{L} (Eq. 4), a supervised learning loss to encourage predicting the ground-truth agent action sequences. Thus our combined objective is:

$$\min_{\theta, \phi, \pi} \lambda_1 \mathcal{L}_{\theta, \phi}^{\text{P}}(\rho) + \lambda_2 \mathcal{L}_{\theta, \phi}^{\text{R}}(\rho) + \lambda_3 \mathcal{L}_{\pi}^{\text{L}}(\rho, \pi), \quad (5)$$

where λ_1 , λ_2 , and λ_3 are hyperparameters controlling the importance of each loss. Optimizing the combination of these losses encourages the program embedding to be both semantically and syntactically informative. More training details can be found in Section L.6.

4.2 Latent Program Search: Synthesizing a Task-Solving Program

Once the program embedding space is learned, our goal becomes searching for a latent program that maximizes the reward described by a given task MDP. To this end, we adapt the Cross Entropy Method (CEM) [65], a gradient-free continuous search algorithm, to iteratively search over the program embedding space. Specifically, we (1) sample a distribution of latent programs, (2) decode the sampled latent programs into programs using the learned program decoder p_{θ} , (3) execute the programs in the task environment and obtain the corresponding rewards, and (4) update the CEM sampling distribution based on the rewards. This process is repeated until either convergence or the maximum number of sampling steps has been reached.

5 Experiments

We first introduce the environment and the tasks in Section 5.1 and describe the experimental setup in Section 5.2. Then, we justify the design of LEAPS by conducting extensive ablation studies in Section 5.3. We describe the baselines used for comparison in Section 5.4, followed by the experimental results presented in Section 5.5. In Section 5.6, we conduct experiments to evaluate the ability of our method to generalize to a larger state space without further learning. Finally, we investigate how LEAPS’ interpretability can be leveraged by conducting experiments that allow humans to debug and improve the programs synthesized by LEAPS in Section 5.7

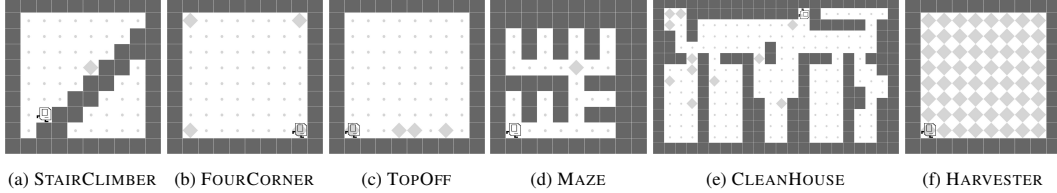


Figure 3: **The Karel problem set**: the domain features an agent navigating through a gridworld with walls and interacting with markers, allowing for designing tasks that demand certain behaviors. The tasks are further described in Section K with visualizations in Figure 15.

5.1 Karel domain

To evaluate the proposed framework, we consider the Karel domain [23], as featured in [17, 19, 21], which features an agent navigating through a gridworld with walls and interacting with markers. The agent has 5 actions for moving and interacting with marker and 5 perceptions for detecting obstacles and markers. The tasks of interest are shown in Figure 3. Note that most tasks have randomly sampled agent, wall, marker, and/or goal configurations. When either training or evaluating, we randomly sample initial configurations upon every episode reset. More details can be found in Section K.

5.2 Programs

To produce programs for learning the program embedding space, we randomly generated a dataset of 50,000 unique programs. Note that the programs are generated independently of any Karel tasks; each program is created only by sampling tokens from the DSL, similar to the procedures used in [16–19, 21, 22]. This dataset is split into a training set with 35,000 programs a validation set with 7,500 programs, and a testing set with 7,500 programs. The validation set is used to select the learned program embedding space to use for the program synthesis stage.

For each program, we sample random Karel states and execute the program on them from different starting states to obtain 10 environment rollouts to compute the program behavior reconstruction loss \mathcal{L}^R and the latent behavior reconstruction loss \mathcal{L}^L when learning the program embedding space. We perform checks to ensure rollouts cover all execution branches in the program so that they are representative of all aspects of the program’s behavior. The maximum length of the programs is 44 tokens and the average length is 17.9. We plot a histogram of their lengths in Figure 14 (in Appendix). More dataset generation details can be found in Section J.

5.3 Ablation Study

We first ablate various components of our proposed framework in order to (1) justify the necessity of the proposed two-stage learning scheme and (2) identify the effects of the proposed objectives. We consider the following baselines and ablations of our method (illustrated Section I).

- Naïve: a program synthesis baseline that learns to directly synthesize a program from scratch by recurrently predicting a sequence of program tokens. This baseline investigates if an end-to-end learning method can solve the problem. More details can be found in Section L.4.
- LEAPS-P: the simplest ablation of LEAPS, in which the program embedding space is learned by only optimizing the program reconstruction loss \mathcal{L}^P (Eq. 1).
- LEAPS-P+R: an ablation of LEAPS which optimizes both the program reconstruction loss \mathcal{L}^P (Eq. 1) and the program behavior reconstruction loss \mathcal{L}^R (Eq. 2).
- LEAPS-P+L: an ablation of LEAPS which optimizes both the program reconstruction loss \mathcal{L}^P (Eq. 1) and the latent behavior reconstruction loss \mathcal{L}^L (Eq. 4).
- LEAPS (LEAPS-P+R+L): LEAPS with all the losses, optimizing our full objective in Eq. 5.
- LEAPS-rand- $\{8/64\}$: similar to LEAPS, this ablation also optimizes the full objective (Eq. 5) for learning the program embedding space. Yet, when searching latent programs, instead of CEM, it simply randomly samples 8/64 candidate latent programs and chooses the best performing one. These baselines justify the effectiveness of using CEM for searching latent programs.

Table 1: Program behavior reconstruction rewards (standard deviations) across all methods.

	WHILE	IFELSE+WHILE	2IF+IFELSE	WHILE+2IF+IFELSE	Avg Reward
Naïve	0.65 (0.33)	0.83 (0.07)	0.61 (0.33)	0.16 (0.06)	0.56
LEAPS-P	0.95 (0.13)	0.82 (0.08)	0.58 (0.35)	0.33 (0.17)	0.67
LEAPS-P+R	0.98 (0.09)	0.77 (0.05)	0.63 (0.25)	0.52 (0.27)	0.72
LEAPS-P+L	1.06 (0.00)	0.84 (0.10)	0.77 (0.23)	0.33 (0.13)	0.75
LEAPS-rand-8	0.62 (0.24)	0.49 (0.09)	0.36 (0.18)	0.28 (0.14)	0.44
LEAPS-rand-64	0.78 (0.22)	0.63 (0.09)	0.55 (0.20)	0.37 (0.09)	0.58
LEAPS	1.06 (0.08)	0.87 (0.13)	0.85 (0.30)	0.57 (0.23)	0.84

Program Behavior Reconstruction. To determine the effectiveness of the proposed two-stage learning scheme and the learning objectives, we measure how effective each ablation is at reconstructing the behaviors of input programs. We use programs from the test set (shown in Figure 9 in Appendix), and utilize the environment state matching reward $R_{\text{mat}}(\hat{\rho}, \rho)$ (Eq. 3), with a 0.1 bonus for synthesizing a syntactically correct program. Thus the return ranges between $[0, 1.1]$. We report the mean cumulative return, over 5 random seeds, of the final programs after convergence.

The results are reported in Table 1. Each test is named after its control flows (*e.g.* IFELSE+WHILE has an if-else statement and a while loop). The naïve program synthesis baseline fails on the complex WHILE+2IF+IFELSE program, as it rarely synthesizes conditional and loop statements, instead generating long sequences of action tokens that attempt to replicate the desired behavior of those statements (see synthesized programs in Figure 10). We believe that this is because it is incentivized to initially predict action tokens to gain more immediate reward, making it less likely to synthesize other tokens. LEAPS and its variations perform better and synthesize more complex programs, demonstrating the importance of the proposed two-stage learning scheme in biasing program search. We also note that LEAPS-P achieves the worst performance out of the CEM search LEAPS ablations, indicating that optimizing the program reconstruction loss \mathcal{L}^P (the VAE loss) alone does not yield satisfactory results. Jointly optimizing \mathcal{L}^P with either the program behavior reconstruction loss \mathcal{L}^R or the latent behavior reconstruction loss \mathcal{L}^L improves the performance, and optimizing our full objective with all three achieves the best performance across all tasks, indicating the effectiveness of the proposed losses. Finally, LEAPS outperforms LEAPS-rand-8/64, suggesting the necessity of adopting better search algorithms such as CEM.

Program Embedding Space Smoothness.

We investigate if the program and latent behavior reconstruction losses encourage learning a behaviorally smooth embedding space. To quantify behavioral smoothness, we measure how much a change in the embedding space corresponds to a change in behavior by comparing execution traces. For all programs we compute the pairwise Euclidean distance between their embeddings in each model. We then calculate the environment state matching distance R_{mat} between the decoded programs by executing them from the same initial state.

The results are reported in Table 2. LEAPS and LEAPS-P+L perform the best, suggesting that optimizing the latent behavior reconstruction objective \mathcal{L}^L , in Eq. 4, is essential for improving the smoothness of the latent space in terms of execution behavior. We further analyze and visualize the learned program embedding space in Section A and Figure 4 (in Appendix).

Table 2: Program embedding space smoothness. For each program, we execute the ten nearest programs in the learned embedding space of each model to calculate the mean state-matching reward R_{mat} against the original program. We report R_{mat} averaged over all programs in each dataset.

	LEAPS-P	LEAPS-P+R	LEAPS-P+L	LEAPS
TRAINING	0.22	0.22	0.31	0.31
VALIDATION	0.22	0.21	0.27	0.27
TESTING	0.22	0.22	0.28	0.27

5.4 Baselines

We evaluate LEAPS against the following baselines (illustrated in Figure 13 in Appendix Section D).

- DRL: a neural network policy trained on each task and taking raw states (Karel grids) as input.
- DRL-abs: a recurrent neural network policy directly trained on each Karel task but taking *abstract* states as input (*i.e.* it sees the same perceptions as LEAPS, *e.g.* `frontIsClear() == true`).
- DRL-abs-t: a DRL transfer learning baseline in which for each task, we train DRL-abs policies on all other tasks, then fine-tune them on the current task. Thus it acquires a prior by learning to

Table 3: Mean return (standard deviation) of all methods across Karel tasks, evaluated over 5 random seeds. DRL methods, program synthesis baselines, and LEAPS ablations are separately grouped.

	STAIRCLIMBER	FOURCORNER	TOPOFF	MAZE	CLEANHOUSE	HARVESTER
DRL	1.00 (0.00)	0.29 (0.05)	0.32 (0.07)	1.00 (0.00)	0.00 (0.00)	0.90 (0.10)
DRL-abs	0.13 (0.29)	0.36 (0.44)	0.63 (0.23)	1.00 (0.00)	0.01 (0.02)	0.32 (0.18)
DRL-abs-t	0.00 (0.00)	0.05 (0.10)	0.17 (0.11)	1.00 (0.00)	0.01 (0.02)	0.16 (0.18)
HRL	-0.51 (0.17)	0.01 (0.00)	0.17 (0.11)	0.62 (0.05)	0.01 (0.00)	0.00 (0.00)
HRL-abs	-0.05 (0.07)	0.00 (0.00)	0.19 (0.12)	0.56 (0.03)	0.00 (0.00)	-0.03 (0.02)
Naïve	0.40 (0.49)	0.13 (0.15)	0.26 (0.27)	0.76 (0.43)	0.07 (0.09)	0.21 (0.25)
VIPER	0.02 (0.02)	0.40 (0.42)	0.30 (0.06)	0.69 (0.05)	0.00 (0.00)	0.51 (0.07)
LEAPS-rand-8	0.10 (0.17)	0.10 (0.14)	0.28 (0.05)	0.40 (0.50)	0.00 (0.00)	0.07 (0.06)
LEAPS-rand-64	0.18 (0.40)	0.20 (0.11)	0.33 (0.07)	0.58 (0.41)	0.03 (0.06)	0.12 (0.05)
LEAPS	1.00 (0.00)	0.45 (0.40)	0.81 (0.07)	1.00 (0.00)	0.18 (0.14)	0.45 (0.28)

first solve other Karel tasks. Rewards are reported for the policies from the task that transferred with highest return. We only transfer DRL-abs policies as some tasks have different state spaces.

- HRL: a hierarchical RL baseline in which a VAE is first trained on action sequences from program execution traces used by LEAPS. Once trained, the decoder is utilized as a low-level policy for learning a high-level policy to sample actions from. Similar to LEAPS, this baseline utilizes the dataset to produce a prior of the domain. It takes raw states (Karel grids) as input.
- HRL-abs: the same method as HRL but taking abstract states (*i.e.* local perceptions) as input.
- VIPER [12]: A decision-tree programmatic policy which imitates the behavior of a deep RL teacher policy via a modified DAgger algorithm [66]. This decision tree policy cannot synthesize loops, allowing us to highlight the performance advantages of more expressive program representation that LEAPS is able to take advantage of.

All the baselines are trained with PPO [67] or SAC [68], including the VIPER teacher policy. More training details can be found in Section L.

5.5 Results

We present the results of the baselines and our method evaluated on the Karel task set based on the environment rewards in Table 3. The reward functions are sparse for all tasks, and are normalized such that the final cumulative return is within $[-1, 1]$ for tasks with penalties and $[0, 1]$ for tasks without; reward functions for each task are detailed in Section K.

Overall Task Performance. Across all but one task, LEAPS yields the best performance. The LEAPS-rand baselines perform significantly worse than LEAPS on all Karel tasks, demonstrating the need for using a search algorithm like CEM during synthesis. The performance of VIPER is bounded by its RL teacher policy, and therefore is outperformed by the DRL baselines on most of the tasks. Meanwhile, DRL-abs-t is generally unable to improve upon DRL-abs across the board, suggesting that transferring Karel behaviors with RL from one task to another is ineffective. Furthermore, both the HRL baselines achieve poor performance, likely because agent actions alone provide insufficient supervision for a VAE to encode useful action trajectories on unseen tasks—unlike programs. Finally, the poor performance of the naïve program synthesis baseline highlights the difficulty and inefficiency of learning to synthesize programs from scratch using only rewards. In the appendix, we present programs synthesized by LEAPS in Figure 11, example optimal programs for each task in Section F (Figure 9), rollout visualizations in Figure 16, and additional results analysis in Section H.

Repetitive Behaviors. Solving STAIRCLIMBER and FOURCORNER requires acquiring repetitive (or looping) behaviors. STAIRCLIMBER, which can be solved by repeating a short, 4-step stair-climbing behavior until the goal marker is reached, is not solved by DRL-abs. LEAPS fully solves the task given the same perceptions, as this behavior can be simply represented with a while loop that repeats the stair-climbing skill. However VIPER performs poorly as its decision tree cannot represent such loops. Similarly, the baselines are unable to perform as well on FOURCORNER, a task in which the agent must pickup a marker located in each corner of the grid. This behavior takes at least 14 timesteps to complete, but can be represented by two nested loops. Similar to STAIRCLIMBER, the bias introduced by the DSL and our generated dataset (which includes nested loops), results in LEAPS being able to perform much better.

Exploration. TOPOFF rewards the agent for adding markers to locations with existing markers. However, there are no restrictions for the agent to wander elsewhere around the environment, thus making exploration a problem for the RL baselines, and thereby also constraining VIPER. LEAPS performs best on this task, as the ground-truth program can be represented by a simple loop that just moves forward and places markers when a marker is detected. MAZE also involves exploration, however its small size (8×8) results in many methods, including LEAPS, solving the task.

Complexity. Solving HARVESTER and CLEANHOUSE requires acquiring complex behaviors, resulting in poor performance from all methods. CLEANHOUSE requires an agent to navigate through a house and pick up all markers along the walls on the way. This requires repeated execution of a skill, of varied length, which navigates around the house, turns into rooms, and picks up markers. As such, all baselines perform very poorly. However, LEAPS is able to perform substantially better because these behaviors can be represented by a program of medium complexity with a while loop and some nested conditional statements. On the other hand, HARVESTER involves simply navigating to and picking up a marker on every spot on the grid. However, this is a difficult program to synthesize given our random dataset generation process; the program we manually derive to solve HARVESTER is long and more syntactically complex than most training programs. As a result, DRL and VIPER outperform LEAPS on this task.

Learned Program Embedding Space. More analysis on our learned program embedding space can be found in the appendix. We present CEM search trajectory visualizations in Section B, demonstrating how the search population’s rewards change over time. To qualitatively investigate the smoothness of the learned program embedding space, we linearly interpolate between pairs of latent programs and display their corresponding decoded programs in Section C. In Section D, we illustrate how predicted programs evolve over the course of CEM search.

5.6 Generalization

We are also interested in learning whether the baselines and the programs synthesized by LEAPS can generalize to novel scenarios without further learning. Specifically, we investigate how well they can generalize to larger state spaces. We expand both STAIRCLIMBER and MAZE to 100×100 grid sizes (from 12×12 and 8×8 , respectively). We directly evaluate the policies or programs obtained from the original tasks with smaller state spaces for all methods except DRL (its observation space changes), which we retrain from scratch. The results are shown in Table 4. All baselines perform significantly worse than before on both tasks. On the contrary, the programs synthesized by LEAPS for the smaller task instances achieve zero-shot generalization to larger task instances without losing any performance. Larger grid size experiments for the other Karel tasks and additional unseen configuration experiments can be found in Section G.

Table 4: Rewards on 100×100 grids.

	STAIRCLIMBER	MAZE
DRL	0.00 (0.00)	0.00 (0.00)
DRL-abs	0.00 (0.00)	0.04 (0.05)
VIPER	0.00 (0.00)	0.10 (0.12)
LEAPS	1.00 (0.00)	1.00 (0.00)

5.7 Interpretability

Interpretability in machine learning [69, 70] is particularly crucial when it comes to learning a policy that interacts with the environment [71–78]. The proposed framework produces programmatic policies that are interpretable from the following aspects as outlined in [70].

- **Trust:** interpretable machine learning methods and models may more easily be trusted since humans tend to be reluctant to trust systems that they do not understand. Programs synthesized by LEAPS can naturally be better trusted since one can simply read and interpret them.
- **Contestability:** the program execution traces produce a chain of reasoning for each action, providing insights on the induced behaviors and thus allowing for contesting improper decisions.
- **Safety:** synthesizing readable programs allows for diagnosing issues earlier (*i.e.* before execution) and provides opportunities to intervene, which is especially critical for safety-critical tasks.

In the rest of this section, we investigate how the proposed framework enjoys interpretability from the three aforementioned aspects. Specifically, synthesized programs are not only readable to human users but also interactive, allowing non-expert users with a basic understanding of programming to diagnose and make edits to improve their performance. To demonstrate this, we asked non-expert

humans to read, interpret, and edit suboptimal LEAPS policies to improve their performance. Participants edited LEAPS programs on 3 Karel tasks with suboptimal reward: TOPOFF, FOURCORNER, and HARVESTER. With just 3 edits, participants obtained a mean reward improvement of 97.1%, and with 5 edits, participants improved it by 125%. This justifies how our synthesized policies can be manually diagnosed and improved, a property which DRL methods lack. More details and discussion can be found in Section E.

6 Discussion

We propose a framework for solving tasks described by MDPs by producing programmatic policies that are more interpretable and generalizable than neural network policies learned by deep reinforcement learning methods. Our proposed framework adopts a flexible program representation and requires only minimal supervision compared to prior programmatic reinforcement learning and program synthesis works. Our proposed two-stage learning scheme not only alleviates the difficulty of learning to synthesize programs from scratch but also enables reusing its learned program embedding space for various tasks. The experiments demonstrate that our proposed framework outperforms DRL and programmatic baselines on a set of Karel tasks by producing expressive and generalizable programs that can consistently solve the tasks. Ablation studies justify the necessity of the proposed two-stage learning scheme as well as the effectiveness of the proposed learning objectives.

While the proposed framework achieves promising results, we would like to acknowledge two assumptions that are implicitly made in this work. First, we assume the existence of a program executor that can produce execution traces of programs. This program executor needs to be able to return perceptions from the environment state as well as apply actions to the environment. While this assumption is widely made in program synthesis works, a program executor can still be difficult to obtain when it comes to real-world robotic tasks. Fortunately, in research fields such as computer vision or robotics, a great amount of effort has been put into satisfying this assumption such as designing modules that can return high-level abstraction of raw sensory input (*e.g.* with object detection networks, proximity/tactile sensors, etc.).

Secondly, we assume that it is possible to generate a distribution of programs whose behaviors are at least remotely related to the desired behaviors for solving the tasks of interest. It can be difficult to synthesize programs which represent behaviors that are more complex than ones in the training program distribution, although one possible solution is to employ a better program generation process to generate programs that induce more complex behaviors. Also, the choice of DSL plays an important role in how complex the programs can be. Ideally, employing a more complex DSL would allow our proposed framework to synthesize more advanced agent behaviors.

In the future, we hope to extend the proposed framework to more challenging domains such as real-world robotics. We believe this framework would allow for deploying robust, interpretable policies for safety-critical tasks such as robotic surgeries. One way to make LEAPS applicable to robotics domains would be to simultaneously learn perception modules and action controllers. Other possible solutions include incorporating program execution methods [79–84] that are designed to allow program execution or designing DSLs that allow pre-training of perception modules and action controllers. Also, the proposed framework shares some characteristics with works in multi-task RL [79, 80, 85–89] and meta-learning [90–99]. Specifically, it learns a program embedding space from a distribution of tasks/programs. Once the program embedding space is learned, it can be reused to solve different tasks without retraining.

Yet, extending LEAPS to such domains can potentially lead to some negative societal impacts. For example, our framework can still capture unintended bias during learning or suffer from adversarial attacks. Furthermore, policies deployed in the real world can create great economic impact by causing job losses in some sectors. Therefore, we would encourage further work to investigate the biases, safety issues, and potential economic impacts to ensure that the deployment in the field does not cause far-reaching, negative societal impacts.

Acknowledgments

The authors appreciate the fruitful discussions with Karl Pertsch, Youngwoon Lee, Ayush Jain, and Grace Zhang. The authors would like to thank Ting-Yu S. Su for contributing to the learned

program embedding spaces visualizations. The authors are grateful to Sidhant Kaushik, Laura Smith, and Siddharth Verma for offering their time to participate in the human debugging interpretability experiment.

Funding Transparency Statement

This project was partially supported by USC startup funding and by NAVER AI Lab.

References

- [1] Volodymyr Mnih, Koray Kavukcuoglu, David Silver, Andrei A. Rusu, Joel Veness, Marc G. Bellemare, Alex Graves, Martin Riedmiller, Andreas K. Fidjeland, Georg Ostrovski, Stig Petersen, Charles Beattie, Amir Sadik, Ioannis Antonoglou, Helen King, Dharshan Kumaran, Daan Wierstra, Shane Legg, and Demis Hassabis. Human level control through deep reinforcement learning. *Nature*, 2015.
- [2] David Silver, Aja Huang, Chris J Maddison, Arthur Guez, Laurent Sifre, George Van Den Driessche, Julian Schrittwieser, Ioannis Antonoglou, Veda Panneershelvam, Marc Lanctot, et al. Mastering the game of go with deep neural networks and tree search. *Nature*, 2016.
- [3] David Silver, Thomas Hubert, Julian Schrittwieser, Ioannis Antonoglou, Matthew Lai, Arthur Guez, Marc Lanctot, Laurent Sifre, Dharshan Kumaran, Thore Graepel, et al. A general reinforcement learning algorithm that masters chess, shogi, and go through self-play. *Science*, 2018.
- [4] Oriol Vinyals, Igor Babuschkin, Wojciech M Czarnecki, Michaël Mathieu, Andrew Dudzik, Junyoung Chung, David H Choi, Richard Powell, Timo Ewalds, Petko Georgiev, et al. Grandmaster level in starcraft ii using multi-agent reinforcement learning. *Nature*, 2019.
- [5] Alexandre Campeau-Lecours, Hugo Lamontagne, Simon Latour, Philippe Fautoux, Véronique Maheu, François Boucher, Charles Deguire, and Louis-Joseph Caron L’Ecuyer. Kinova modular robot arms for service robotics applications. In *Rapid Automation: Concepts, Methodologies, Tools, and Applications*. 2019.
- [6] Shixiang Gu, Ethan Holly, Timothy Lillicrap, and Sergey Levine. Deep reinforcement learning for robotic manipulation with asynchronous off-policy updates. In *International Conference on Robotics and Automation*, 2017.
- [7] OpenAI: Marcin Andrychowicz, Bowen Baker, Maciek Chociej, Rafal Jozefowicz, Bob McGrew, Jakub Pachocki, Arthur Petron, Matthias Plappert, Glenn Powell, Alex Ray, et al. Learning dexterous in-hand manipulation. *The International Journal of Robotics Research*, 2020.
- [8] Danijar Hafner, Timothy Lillicrap, Jimmy Ba, and Mohammad Norouzi. Dream to control: Learning behaviors by latent imagination. In *International Conference on Learning Representations*, 2020.
- [9] Jun Yamada, Youngwoon Lee, Gautam Salhotra, Karl Pertsch, Max Pflueger, Gaurav S Sukhatme, Joseph J Lim, and Peter Englert. Motion planner augmented reinforcement learning for robot manipulation in obstructed environments. In *Conference on Robot Learning*, 2020.
- [10] Grace Zhang, Linghan Zhong, Youngwoon Lee, and Joseph J Lim. Policy transfer across visual and dynamics domain gaps via iterative grounding. In *Robotics: Science and Systems*, 2021.
- [11] Youngwoon Lee, Edward S Hu, Zhengyu Yang, and Joseph J Lim. To follow or not to follow: Selective imitation learning from observations. In *Conference on Robot Learning*, 2019.
- [12] Osbert Bastani, Yewen Pu, and Armando Solar-Lezama. Verifiable reinforcement learning via policy extraction. In *Neural Information Processing Systems*, 2018.

- [13] Jeevana Priya Inala, Osbert Bastani, Zenna Tavares, and Armando Solar-Lezama. Synthesizing programmatic policies that inductively generalize. In *International Conference on Learning Representations*, 2020.
- [14] Abhinav Verma, Vijayaraghavan Murali, Rishabh Singh, Pushmeet Kohli, and Swarat Chaudhuri. Programmatically interpretable reinforcement learning. In *International Conference on Machine Learning*, 2018.
- [15] Abhinav Verma, Hoang Le, Yisong Yue, and Swarat Chaudhuri. Imitation-projected programmatic reinforcement learning. In *Neural Information Processing Systems*, 2019.
- [16] Jacob Devlin, Jonathan Uesato, Surya Bhupatiraju, Rishabh Singh, Abdel-rahman Mohamed, and Pushmeet Kohli. Robustfill: Neural program learning under noisy i/o. In *International Conference on Machine Learning*, 2017.
- [17] Rudy R Bunel, Matthew Hausknecht, Jacob Devlin, Rishabh Singh, and Pushmeet Kohli. Leveraging grammar and reinforcement learning for neural program synthesis. In *International Conference on Learning Representations*, 2018.
- [18] Xinyun Chen, Chang Liu, and Dawn Song. Execution-guided neural program synthesis. In *International Conference on Learning Representations*, 2019.
- [19] Eui Chul Shin, Illia Polosukhin, and Dawn Song. Improving neural program synthesis with inferred execution traces. In *Neural Information Processing Systems*, 2018.
- [20] Miguel Lázaro-Gredilla, Dianhuan Lin, J Swaroop Guntupalli, and Dileep George. Beyond imitation: Zero-shot task transfer on robots by learning concepts as cognitive programs. *Science Robotics*, 2019.
- [21] Shao-Hua Sun, Hyeonwoo Noh, Sriram Somasundaram, and Joseph Lim. Neural program synthesis from diverse demonstration videos. In *International Conference on Machine Learning*, 2018.
- [22] Raphaël Dang-Nhu. Plans: Neuro-symbolic program learning from videos. In H. Larochelle, M. Ranzato, R. Hadsell, M. F. Balcan, and H. Lin, editors, *Neural Information Processing Systems*, 2020.
- [23] Richard E Pattis. *Karel the robot: a gentle introduction to the art of programming*. John Wiley & Sons, Inc., 1981.
- [24] Danfei Xu, Suraj Nair, Yuke Zhu, Julian Gao, Animesh Garg, Li Fei-Fei, and Silvio Savarese. Neural task programming: Learning to generalize across hierarchical tasks. In *International Conference on Robotics and Automation*, 2018.
- [25] Jacob Devlin, Rudy R Bunel, Rishabh Singh, Matthew Hausknecht, and Pushmeet Kohli. Neural program meta-induction. In *Advances in Neural Information Processing Systems*, 2017.
- [26] Arvind Neelakantan, Quoc V Le, and Ilya Sutskever. Neural programmer: Inducing latent programs with gradient descent. In *International Conference on Learning Representations*, 2015.
- [27] Alex Graves, Greg Wayne, and Ivo Danihelka. Neural turing machines. *arXiv preprint arXiv:1410.5401*, 2014.
- [28] Łukasz Kaiser and Ilya Sutskever. Neural gpu learn algorithms. In *International Conference on Learning Representations*, 2016.
- [29] Alexander L. Gaunt, Marc Brockschmidt, Nate Kushman, and Daniel Tarlow. Differentiable programs with neural libraries. In *International Conference on Machine Learning*, 2017.
- [30] Scott Reed and Nando De Freitas. Neural programmer-interpreters. In *International Conference on Learning Representations*, 2016.
- [31] Jonathon Cai, Richard Shin, and Dawn Song. Making neural programming architectures generalize via recursion. In *International Conference on Learning Representations*, 2017.

- [32] Da Xiao, Jo-Yu Liao, and Xingyuan Yuan. Improving the universality and learnability of neural programmer-interpreters with combinator abstraction. In *International Conference on Learning Representations*, 2018.
- [33] Michael Burke, Svetlin Penkov, and Subramanian Ramamoorthy. From explanation to synthesis: Compositional program induction for learning from demonstration. *arXiv preprint arXiv:1902.10657*, 2019.
- [34] Yujun Yan, Kevin Swersky, Danai Koutra, Parthasarathy Ranganathan, and Milad Hashemi. Neural execution engines: Learning to execute subroutines. In *Neural Information Processing Systems*, 2020.
- [35] Yujia Li, Felix Gimeno, Pushmeet Kohli, and Oriol Vinyals. Strong generalization and efficiency in neural programs. *arXiv preprint arXiv:2007.03629*, 2020.
- [36] De-An Huang, Suraj Nair, Danfei Xu, Yuke Zhu, Animesh Garg, Li Fei-Fei, Silvio Savarese, and Juan Carlos Niebles. Neural task graphs: Generalizing to unseen tasks from a single video demonstration. In *IEEE Conference on Computer Vision and Pattern Recognition*, 2019.
- [37] Matko Bošnjak, Tim Rocktäschel, Jason Naradowsky, and Sebastian Riedel. Programming with a differentiable forth interpreter. In *International Conference on Machine Learning*, 2017.
- [38] Emilio Parisotto, Abdel-rahman Mohamed, Rishabh Singh, Lihong Li, Dengyong Zhou, and Pushmeet Kohli. Neuro-symbolic program synthesis. In *International Conference on Learning Representations*, 2017.
- [39] Richard Shin, Illia Polosukhin, and Dawn Song. Improving neural program synthesis with inferred execution traces. In *Neural Information Processing Systems*, 2018.
- [40] Yunchao Liu, Jiajun Wu, Zheng Wu, Daniel Ritchie, William T. Freeman, and Joshua B. Tenenbaum. Learning to describe scenes with programs. In *International Conference on Learning Representations*, 2019.
- [41] Xi Victoria Lin, Chenglong Wang, Luke Zettlemoyer, and Michael D Ernst. NI2bash: A corpus and semantic parser for natural language interface to the linux operating system. In *International Conference on Language Resources and Evaluation*, 2018.
- [42] Yuan-Hong Liao, Xavier Puig, Marko Boben, Antonio Torralba, and Sanja Fidler. Synthesizing environment-aware activities via activity sketches. In *IEEE Conference on Computer Vision and Pattern Recognition*, 2019.
- [43] Kevin Ellis, Maxwell Nye, Yewen Pu, Felix Sosa, Josh Tenenbaum, and Armando Solar-Lezama. Write, execute, assess: Program synthesis with a repl. In *Neural Information Processing Systems*, 2019.
- [44] Kevin Ellis, Catherine Wong, Maxwell Nye, Mathias Sable-Meyer, Luc Cary, Lucas Morales, Luke Hewitt, Armando Solar-Lezama, and Joshua B Tenenbaum. Dreamcoder: Growing generalizable, interpretable knowledge with wake-sleep bayesian program learning. *arXiv preprint arXiv:2006.08381*, 2020.
- [45] Matej Balog, Alexander L Gaunt, Marc Brockschmidt, Sebastian Nowozin, and Daniel Tarlow. Deepcoder: Learning to write programs. In *International Conference on Learning Representations*, 2017.
- [46] Paweł Liskowski, Krzysztof Krawiec, Nihat Engin Toklu, and Jerry Swan. Program synthesis as latent continuous optimization: Evolutionary search in neural embeddings. In *Genetic and Evolutionary Computation Conference*, 2020.
- [47] Daniel A Abolafia, Mohammad Norouzi, Jonathan Shen, Rui Zhao, and Quoc V Le. Neural program synthesis with priority queue training. *arXiv preprint arXiv:1801.03526*, 2018.
- [48] Joey Hong, David Dohan, Rishabh Singh, Charles Sutton, and Manzil Zaheer. Latent programmer: Discrete latent codes for program synthesis. In *International Conference on Machine Learning*, 2021.

- [49] Tom Silver, Kelsey R Allen, Alex K Lew, Leslie Pack Kaelbling, and Josh Tenenbaum. Few-shot bayesian imitation learning with logical program policies. In *Association for the Advancement of Artificial Intelligence*, 2020.
- [50] Jiajun Wu, Joshua B Tenenbaum, and Pushmeet Kohli. Neural scene de-rendering. In *IEEE Conference on Computer Vision and Pattern Recognition*, 2017.
- [51] Mark Chen, Jerry Tworek, Heewoo Jun, Qiming Yuan, Henrique Ponde, Jared Kaplan, Harri Edwards, Yura Burda, Nicholas Joseph, Greg Brockman, et al. Evaluating large language models trained on code. *arXiv preprint arXiv:2107.03374*, 2021.
- [52] Ferran Alet, Javier Lopez-Contreras, James Koppel, Maxwell Nye, Armando Solar-Lezama, Tomas Lozano-Perez, Leslie Kaelbling, and Joshua Tenenbaum. A large-scale benchmark for few-shot program induction and synthesis. In *International Conference on Machine Learning*, 2021.
- [53] Xinyun Chen, Dawn Song, and Yuandong Tian. Latent execution for neural program synthesis beyond domain-specific languages. *arXiv preprint arXiv:2107.00101*, 2021.
- [54] Jacob Austin, Augustus Odena, Maxwell Nye, Maarten Bosma, Henryk Michalewski, David Dohan, Ellen Jiang, Carrie Cai, Michael Terry, Quoc Le, et al. Program synthesis with large language models. *arXiv preprint arXiv:2108.07732*, 2021.
- [55] Joey Hong, David Dohan, Rishabh Singh, Charles Sutton, and Manzil Zaheer. Latent programmer: Discrete latent codes for program synthesis. In *International Conference on Machine Learning*, 2021.
- [56] Catherine Wong, Kevin Ellis, Joshua B Tenenbaum, and Jacob Andreas. Leveraging language to learn program abstractions and search heuristics. In *International Conference on Machine Learning*, 2021.
- [57] Xinyun Chen, Petros Maniatis, Rishabh Singh, Charles Sutton, Hanjun Dai, Max Lin, and Denny Zhou. Spreadsheetcoder: Formula prediction from semi-structured context. In *International Conference on Machine Learning*, 2021.
- [58] Maxwell Nye, Yewen Pu, Matthew Bowers, Jacob Andreas, Joshua B. Tenenbaum, and Armando Solar-Lezama. Representing partial programs with blended abstract semantics. In *International Conference on Learning Representations*, 2021.
- [59] Dongkyu Choi and Pat Langley. Learning teleoreactive logic programs from problem solving. In *International Conference on Inductive Logic Programming*, 2005.
- [60] Elly Winner and Manuela Veloso. Distill: Learning domain-specific planners by example. In *International Conference on Machine Learning*, 2003.
- [61] Mikel Landajuela, Brenden K Petersen, Sookyung Kim, Claudio P Santiago, Ruben Glatt, Nathan Mundhenk, Jacob F Pettit, and Daniel Faissol. Discovering symbolic policies with deep reinforcement learning. In *International Conference on Machine Learning*, 2021.
- [62] Diederik P Kingma and Max Welling. Auto-encoding variational bayes. In *International Conference on Learning Representations*, 2014.
- [63] Irina Higgins, Loic Matthey, Arka Pal, Christopher Burgess, Xavier Glorot, Matthew Botvinick, Shakir Mohamed, and Alexander Lerchner. beta-vae: Learning basic visual concepts with a constrained variational framework. In *International Conference on Learning Representations*, 2016.
- [64] Ronald J Williams. Simple statistical gradient-following algorithms for connectionist reinforcement learning. *Machine learning*, 1992.
- [65] Reuven Y Rubinstein. Optimization of computer simulation models with rare events. *European Journal of Operational Research*, 1997.

- [66] Stéphane Ross, Geoffrey Gordon, and Drew Bagnell. A reduction of imitation learning and structured prediction to no-regret online learning. In *International Conference on Artificial Intelligence and Statistics*, 2011.
- [67] John Schulman, Filip Wolski, Prafulla Dhariwal, Alec Radford, and Oleg Klimov. Proximal policy optimization algorithms. *arXiv preprint arXiv:1707.06347*, 2017.
- [68] Tuomas Haarnoja, Aurick Zhou, Pieter Abbeel, and Sergey Levine. Soft actor-critic: Off-policy maximum entropy deep reinforcement learning with a stochastic actor. In *International Conference on Machine Learning*, 2018.
- [69] Zachary C Lipton. The mythos of model interpretability. In *ICML Workshop on Human Interpretability in Machine Learning*, 2016.
- [70] Owen Shen. Interpretability in ml: A broad overview, 2020. URL <https://mlu.red/muse/52906366310>.
- [71] Jesse Zhang, Brian Cheung, Chelsea Finn, Sergey Levine, and Dinesh Jayaraman. Cautious adaptation for reinforcement learning in safety-critical settings. In *International Conference on Machine Learning*, 2020.
- [72] Lukas Hewing, Juraj Kabzan, and Melanie N. Zeilinger. Cautious model predictive control using gaussian process regression. *IEEE Transactions on Control Systems Technology*, 2019.
- [73] Jaime F Fisac, Anayo K Akametalu, Melanie N Zeilinger, Shahab Kaynama, Jeremy Gillula, and Claire J Tomlin. A general safety framework for learning-based control in uncertain robotic systems. *IEEE Transactions on Automatic Control*, 2018.
- [74] A. Hakobyan, G. C. Kim, and I. Yang. Risk-aware motion planning and control using cvar-constrained optimization. *IEEE Robotics and Automation Letters*, 2019.
- [75] Dorsa Sadigh and Ashish Kapoor. Safe control under uncertainty with probabilistic signal temporal logic. In *Proceedings of Robotics: Science and Systems*, 2016.
- [76] Felix Berkenkamp, Matteo Turchetta, Angela P. Schoellig, and Andreas Krause. Safe model-based reinforcement learning with stability guarantees. In *Advances in Neural Information Processing Systems*, 2017.
- [77] Brijen Thananjeyan, Ashwin Balakrishna, Ugo Rosolia, Felix Li, Rowan McAllister, Joseph E. Gonzalez, Sergey Levine, Francesco Borrelli, and Ken Goldberg. Safety augmented value estimation from demonstrations (saved): Safe deep model-based rl for sparse cost robotic tasks. *IEEE Robotics and Automation Letters*, 2020.
- [78] Anil Aswani, Humberto Gonzalez, S Shankar Sastry, and Claire Tomlin. Provably safe and robust learning-based model predictive control. *Automatica*, 2013.
- [79] Jacob Andreas, Dan Klein, and Sergey Levine. Modular multitask reinforcement learning with policy sketches. In *International Conference on Machine Learning*, 2017.
- [80] Junhyuk Oh, Satinder Singh, Honglak Lee, and Pushmeet Kohli. Zero-shot task generalization with multi-task deep reinforcement learning. In *International Conference on Machine Learning*, 2017.
- [81] Shao-Hua Sun, Te-Lin Wu, and Joseph J. Lim. Program guided agent. In *International Conference on Learning Representations*, 2020.
- [82] Yichen Yang, Jeevana Priya Inala, Osbert Bastani, Yewen Pu, Armando Solar-Lezama, and Martin Rinard. Program synthesis guided reinforcement learning. *arXiv preprint arXiv:2102.11137*, 2021.
- [83] Youngwoon Lee, Shao-Hua Sun, Sriram Somasundaram, Edward Hu, and Joseph J. Lim. Composing complex skills by learning transition policies. In *International Conference on Learning Representations*, 2019.

- [84] Zelin Zhao, Karan Samel, Binghong Chen, and Le Song. Proto: Program-guided transformer for program-guided tasks. *arXiv preprint arXiv:2110.00804*, 2021.
- [85] Yee Whye Teh, Victor Bapst, Wojciech Marian Czarnecki, John Quan, James Kirkpatrick, Raia Hadsell, Nicolas Heess, and Razvan Pascanu. Distral: Robust multitask reinforcement learning. *arXiv preprint arXiv:1707.04175*, 2017.
- [86] Richard Socher Tianmin Shu, Caiming Xiong. Hierarchical and interpretable skill acquisition in multi-task reinforcement learning. *International Conference on Learning Representations*, 2018.
- [87] Sungryull Sohn, Junhyuk Oh, and Honglak Lee. Hierarchical reinforcement learning for zero-shot generalization with subtask dependencies. In *Advances in Neural Information Processing Systems*, 2018.
- [88] Ayush Jain, Andrew Szot, and Joseph Lim. Generalization to new actions in reinforcement learning. In Hal Daumé III and Aarti Singh, editors, *Proceedings of the 37th International Conference on Machine Learning*, volume 119 of *Proceedings of Machine Learning Research*, pages 4661–4672. PMLR, 13–18 Jul 2020. URL <https://proceedings.mlr.press/v119/jain20b.html>.
- [89] Karl Pertsch, Youngwoon Lee, and Joseph J. Lim. Accelerating reinforcement learning with learned skill priors. In *Conference on Robot Learning*, 2020.
- [90] Jake Snell, Kevin Swersky, and Richard Zemel. Prototypical networks for few-shot learning. In *Advances in Neural Information Processing Systems*. 2017.
- [91] Risto Vuorio, Shao-Hua Sun, Hexiang Hu, and Joseph J Lim. Multimodal model-agnostic meta-learning via task-aware modulation. In *Neural Information Processing Systems*, 2019.
- [92] Oriol Vinyals, Charles Blundell, Tim Lillicrap, Daan Wierstra, et al. Matching networks for one shot learning. In *Advances in Neural Information Processing Systems*, 2016.
- [93] Chelsea Finn, Pieter Abbeel, and Sergey Levine. Model-Agnostic Meta-Learning for Fast Adaptation of Deep Networks. In *International Conference on Machine Learning*, 2017.
- [94] Risto Vuorio, Shao-Hua Sun, Hexiang Hu, and Joseph J Lim. Toward multimodal model-agnostic meta-learning. *arXiv preprint arXiv:1812.07172*, 2018.
- [95] Wei-Yu Chen, Yen-Cheng Liu, Zsolt Kira, Yu-Chiang Frank Wang, and Jia-Bin Huang. A closer look at few-shot classification. In *International Conference on Learning Representations*, 2019.
- [96] Yoonho Lee and Seungjin Choi. Gradient-Based Meta-Learning with Learned Layerwise Metric and Subspace. In *International Conference on Machine Learning*, 2018.
- [97] Alex Nichol and John Schulman. Reptile: a scalable metalearning algorithm. *arXiv preprint arXiv:1803.02999*, 2018.
- [98] Garima Pruthi, Frederick Liu, Satyen Kale, and Mukund Sundararajan. Estimating training data influence by tracing gradient descent. In *Neural Information Processing Systems*, 2020.
- [99] Yun-Chun Chen, Chao-Te Chou, and Yu-Chiang Frank Wang. Learning to learn in a semi-supervised fashion. In *European Conference on Computer Vision*, 2020.
- [100] I.T. Jolliffe. *Principal Component Analysis*. Springer Verlag, 1986.
- [101] Mihalj Bakator and Dragica Radosav. Deep learning and medical diagnosis: A review of literature. *Multimodal Technologies and Interaction*, 2018.
- [102] Dinggang Shen, Guorong Wu, and Heung-Il Suk. Deep learning in medical image analysis. *Annual review of biomedical engineering*, 2017.
- [103] Biraja Ghoshal and Allan Tucker. Estimating uncertainty and interpretability in deep learning for coronavirus (covid-19) detection. *arXiv preprint arXiv:2003.10769*, 2020.

- [104] Chia-Jung Chang, Wei Guo, Jie Zhang, Jon Newman, Shao-Hua Sun, and Matt Wilson. Behavioral clusters revealed by end-to-end decoding from microendoscopic imaging. *bioRxiv*, 2021.
- [105] Amitojdeep Singh, Sourya Sengupta, and Vasudevan Lakshminarayanan. Explainable deep learning models in medical image analysis. *Journal of Imaging*, 2020.
- [106] Vladimir Iosifovich Levenshtein. Binary codes capable of correcting deletions, insertions and reversals. *Soviet Physics Doklady*, 1966.
- [107] Michihiro Yasunaga and Percy Liang. Graph-based, self-supervised program repair from diagnostic feedback. In *International Conference on Machine Learning*, 2020.
- [108] Hoang Duong Thien Nguyen, Dawei Qi, Abhik Roychoudhury, and Satish Chandra. Semfix: Program repair via semantic analysis. In *Conference on Software Engineering*, 2013.
- [109] Jiajun Jiang, Yingfei Xiong, Hongyu Zhang, Qing Gao, and Xiangqun Chen. Shaping program repair space with existing patches and similar code. In *ACM SIGSOFT International Symposium on Software Testing and Analysis*, 2018.
- [110] Qi Xin and Steven P Reiss. Leveraging syntax-related code for automated program repair. In *International Conference on Automated Software Engineering*, 2017.
- [111] Claire Le Goues, Michael Pradel, and Abhik Roychoudhury. Automated program repair. *Communications of the ACM*, 2019.
- [112] Eric Schulte, Stephanie Forrest, and Westley Weimer. Automated program repair through the evolution of assembly code. In *International Conference on Automated Software Engineering*, 2010.
- [113] Anil Koyuncu, Kui Liu, Tegawendé F Bissyandé, Dongsun Kim, Jacques Klein, Martin Monperrus, and Yves Le Traon. Fixminer: Mining relevant fix patterns for automated program repair. *Empirical Software Engineering*, 2020.
- [114] Thomas Durieux and Martin Monperrus. Dynamoth: dynamic code synthesis for automatic program repair. In *International Workshop on Automation of Software Test*, 2016.
- [115] Yi Li, Shaohua Wang, and Tien N Nguyen. Dlfix: Context-based code transformation learning for automated program repair. In *International Conference on Software Engineering*, 2020.
- [116] Liushan Chen, Yu Pei, and Carlo A Furia. Contract-based program repair without the contracts. In *International Conference on Automated Software Engineering*, 2017.
- [117] Martin White, Michele Tufano, Matias Martinez, Martin Monperrus, and Denys Poshyvanyk. Sorting and transforming program repair ingredients via deep learning code similarities. In *IEEE International Conference on Software Analysis, Evolution and Reengineering*, 2019.
- [118] Rahul Gupta, Soham Pal, Aditya Kanade, and Shirish Shevade. Deepfix: Fixing common c language errors by deep learning. In *Association for the Advancement of Artificial Intelligence*, 2017.
- [119] Ke Wang, Rishabh Singh, and Zhendong Su. Dynamic neural program embedding for program repair. *arXiv preprint arXiv:1711.07163*, 2017.
- [120] Ali Mesbah, Andrew Rice, Emily Johnston, Nick Glorioso, and Edward Aftandilian. Deepdelta: learning to repair compilation errors. In *ACM Joint Meeting on European Software Engineering Conference and Symposium on the Foundations of Software Engineering*, 2019.
- [121] He Zhu, Zikang Xiong, Stephen Magill, and Suresh Jagannathan. An inductive synthesis framework for verifiable reinforcement learning. In *ACM SIGPLAN Conference on Programming Language Design and Implementation*, 2019.
- [122] Jonathan Long, Evan Shelhamer, and Trevor Darrell. Fully convolutional networks for semantic segmentation. In *IEEE Conference on Computer Vision and Pattern Recognition*, 2015.

- [123] Karol Hausman, Jost Tobias Springenberg, Ziyu Wang, Nicolas Heess, and Martin Riedmiller. Learning an embedding space for transferable robot skills. In *International Conference on Learning Representations*, 2018.
- [124] Volodymyr Mnih, Koray Kavukcuoglu, David Silver, Andrei A Rusu, Joel Veness, Marc G Bellemare, Alex Graves, Martin Riedmiller, Andreas K Fidjeland, Georg Ostrovski, et al. Human-level control through deep reinforcement learning. *Nature*, 2015.

Appendix

Table of Contents

List of Figures	20
List of Tables	20
A Program Embedding Space Visualizations	21
B Cross Entropy Method Trajectory Visualization	22
C Program Embedding Space Interpolations	25
D Program Evolution	26
E Interpretability: Human Debugging of LEAPS Programs	27
F Optimal and Synthesized Programs	31
F.1 Program Behavior Reconstruction	34
F.2 Karel Environment Tasks	35
G Additional Generalization Experiments	35
G.1 Generalization on FOURCORNER, TOPOFF, and HARVESTER	35
G.2 Generalization to Unseen Configurations	36
H Additional Analysis on Experimental Results	37
H.1 DRL vs. DRL-abs	37
H.2 VIPER generalization	37
I Detailed Descriptions and Illustrations of Ablations and Baselines	37
I.1 Ablations	38
I.2 Baselines	38
J Program Dataset Generation Details	41
K Karel Task Details	41
K.1 STAIRCLIMBER	43
K.2 FOURCORNER	44
K.3 TOPOFF	44
K.4 MAZE	44
K.5 CLEANHOUSE	44
K.6 HARVESTER	44
L Hyperparameters and Training Details	44
L.1 DRL and DRL-abs	44
L.2 DRL-abs-t	45
L.3 HRL	45
L.4 Naïve	46
L.5 VIPER	47
L.6 Program Embedding Space VAE Model	48
L.7 Cross-Entropy Method (CEM)	49
L.8 Random Search LEAPS Ablation	50
M Computational Resources	51

List of Figures

4	Visualizations of Learned Program Embedding Space	22
5	STAIRCLIMBER CEM Trajectory Visualization	23
6	FOURCORNER CEM Trajectory Visualization	24
7	Human Debugging Experiment User Interface	27
8	Human Debugging Experiment Example Programs	29
9	Ground-Truth Test Programs and Karel Programs	31
10	Program Reconstruction Task Synthesized Programs	33
11	LEAPS Karel Tasks Synthesized Programs	34
12	LEAPS Ablations Illustrations	39
13	Baseline Methods Illustrations	40
14	Program Length Histograms	41
15	Karel Task Start/End State Depictions	43
16	Karel Rollout Visualizations	53

List of Tables

5	LEAPS Close Latent Program Interpolation	25
6	LEAPS Far Latent Program Interpolation	25
7	Program Evolution Over CEM Search	26
8	Human Debugging Experiment Results	27
10	Unseen Configurations Performance	36
11	Program Token Generation Probabilities	41
12	LEAPS Length 100 Synthesized Karel Programs	42

A Program Embedding Space Visualizations

In this section, we present and analyze visualizations providing insights on the program embedding spaces learned by LEAPS and its variations. To investigate the learned program embedding space, we perform dimensionality reduction with PCA [100] to embed the following data to a 2D space for visualizations shown in Figure 4:

- Latent programs from the training dataset encoded by a learned encoder q_ϕ , visualized as blue scatters. There are 35k training programs.
- Samples drawn from a normal distribution $\mathcal{N}(0, 1)$, visualized as green scatters. This is to show how a distribution would look like if the embedding space is learned by using a highly weighted KL-divergence penalty (*i.e.* a large β value the VAE loss). We compared this against the latent program distribution learned by our method to justify the effectiveness of the proposed objectives: the program behavior reconstruction loss (\mathcal{L}^R) and the latent behavior reconstruction loss (\mathcal{L}^L).
- Ground-truth (GT) test programs from the testing dataset, encoded by a learned decoder q_ϕ , visualized as plus signs (+) with different colors. We selected 4 test programs.
- Reconstructed programs which are predicted (Pred) by each method given visualized as crosses (\times) with different colors. Since there are 4 test programs selected, 4 reconstructed programs are visualized. Each pair of test program and predicted program is visualized with the same color. These predicted (*i.e.* synthesized) programs are also shown in Figure 10.

Embedding Space Coverage. Even though the testing programs are not in the training program dataset, and therefore are unseen to models, their embedding vectors still lie in the distribution learned by all the models. This indicates that the learned embedding spaces cover a wide distribution of programs.

Latent Program Distribution vs. Normal Distribution. We now compare two distributions: the latent program distribution formed by encoding all the training programs to the program embedding space and a normal distribution $\mathcal{N}(0, 1)$. One can view the normal distribution as the distribution obtained by heavily enforcing the weight of the KL-divergence term when training a VAE model. We discuss the shape of the latent program distribution in the learned program embedding space as follows:

- LEAPS-P: since LEAPS+P simply optimizes the β -VAE loss (the program reconstruction loss \mathcal{L}^P), which puts a lot of emphasis on the KL-divergence term, the shape of the latent program distribution is very similar to a normal distribution as shown in Figure 4 (a).
- LEAPS-P+R: while LEAPS+P+R additionally optimizes the program behavior reconstruction loss \mathcal{L}^R , the shape of the latent program distribution is still similar to a normal distribution, as shown in Figure 4 (b). We hypothesize that it is because the program behavior reconstruction loss alone might not be strong or explicit enough to introduce a change.
- LEAPS-P+L: the shape of the latent program distribution in the program embedding space learned by LEAPS+P+L is significantly different from a normal distribution, as shown in Figure 4 (c). This suggest that employing the latent behavior reconstruction loss \mathcal{L}^L dramatically contributes to the learning. We believe it is because the latent behavior reconstruction loss is optimized with direct gradients and therefore provides a stronger learning signal especially compared to the program behavior reconstruction loss \mathcal{L}^R , which is optimized using REINFORCE [64].
- LEAPS (LEAPS-P+R+L): LEAPS optimizes the full objective that includes all three proposed objectives and form a similar distribution shape as the one learned by LEAPS+P+L. However, the distance between each pair of the ground-truth testing program and the predicted program is much closer in the program embedding space learned by LEAPS compared to the space learned by LEAPS+P+L. This justifies the effectiveness of the proposed program behavior reconstruction loss \mathcal{L}^R , which can bring the programs with similar behaviors closer in the embedding space.

Summary. The visualizations of the program embedding spaces learned by LEAPS and its ablations qualitatively justify the effectiveness of the proposed learning objectives, as complementary to the quantitative results presented in the main paper.

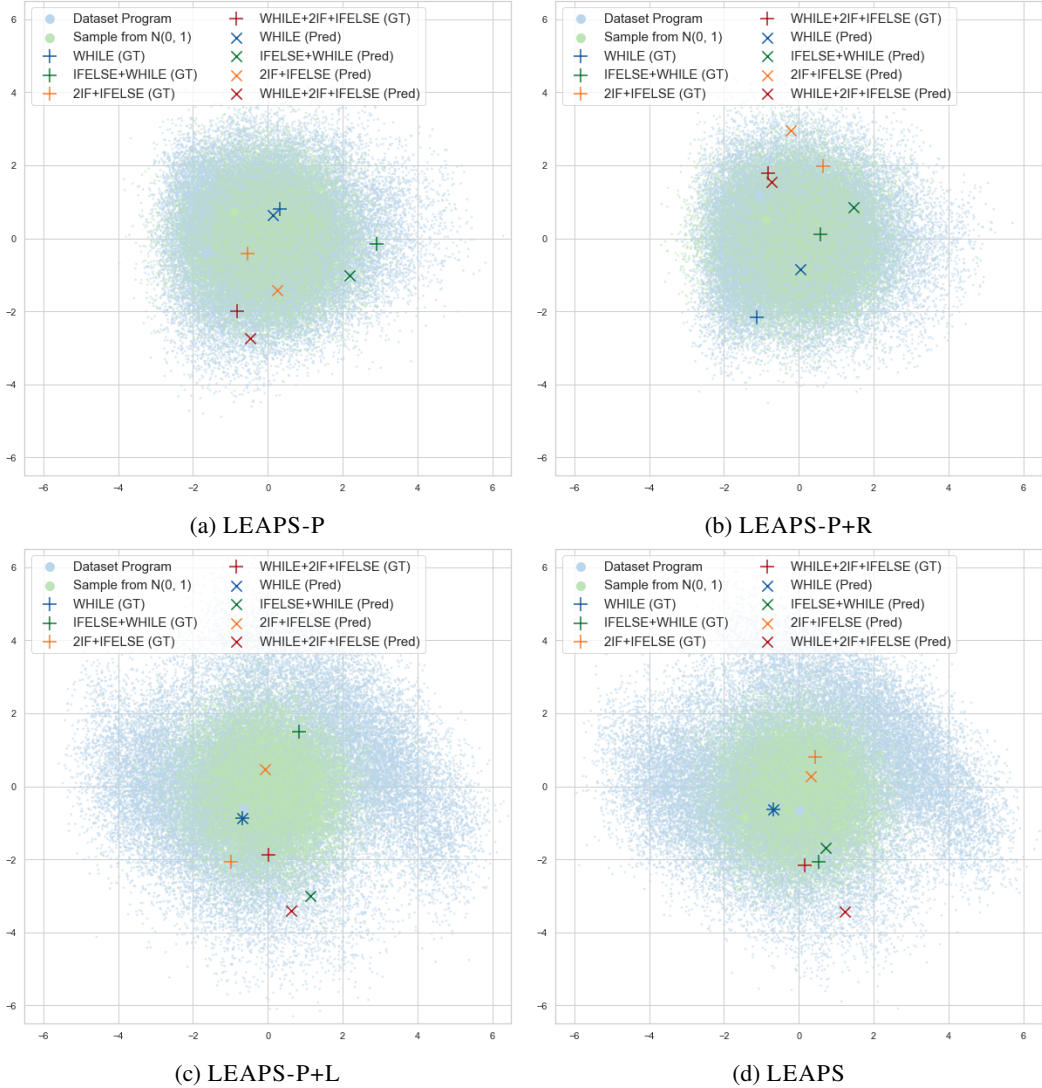


Figure 4: **Visualizations of learned program embedding space.** We perform dimensionality reduction with PCA to embed encoded programs from the training dataset, samples drawn from a normal distribution, programs from the testing dataset, and programs reconstructed by models to a 2D space. The shape of the latent training programs in the program embedding spaces learned by LEAPS-P and LEAPS-P+R are similar to a normal distribution, while in the program embedding spaces learned by LEAPS and LEAPS-P+L, the shape is more twisted, suggesting the effectiveness of the proposed latent behavior reconstruction objective. Moreover, the distances between pairs of ground-truth programs and their reconstructions are smaller in the program embedding space learned by LEAPS, highlighting the advantage of employing both of the two proposed behavior reconstruction objectives.

B Cross Entropy Method Trajectory Visualization

As described in the main paper, once the program embedding space is learned by LEAPS, our goal becomes searching for a latent program that maximizes the reward described by a given task MDP. To this end, we adapt the Cross Entropy Method (CEM) [65], a gradient-free continuous search algorithm, to iteratively search over the program embedding space. Specifically, we iteratively perform the following steps:

1. Sample a distribution of candidate latent programs.

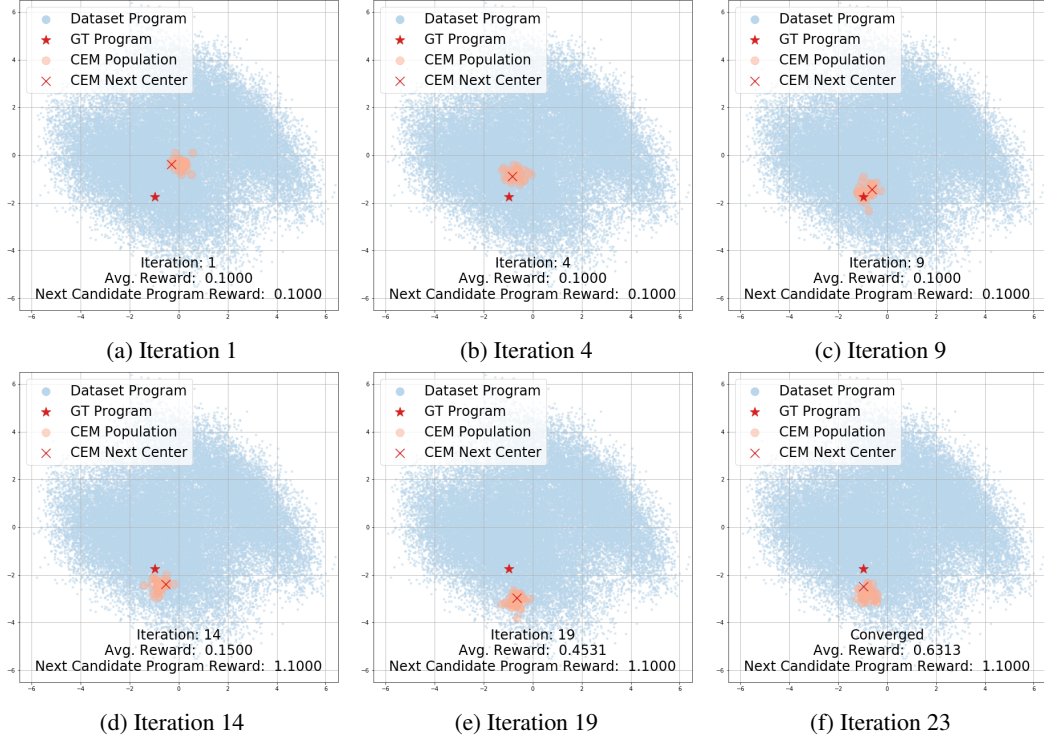


Figure 5: STAIRCLIMBER CEM Trajectory Visualization. Latent training programs from the training dataset, a ground-truth program for STAIRCLIMBER task, CEM populations, and CEM next candidate programs are embedded to a 2D space using PCA. Both the average reward of the entire population and the reward of the next candidate program (CEM Next Center) consistently increase as the number of iterations increase. Also, the CEM population gradually moves toward where the ground-truth program is located.

2. Decode the sampled latent programs into programs using the learned program decoder p_θ .
3. Execute the programs in the task environment and obtain the corresponding rewards.
4. Update the CEM sampling distribution based on the rewards.

This process is repeated until either convergence or the maximum number of sampling steps has been reached.

We perform dimensionality reduction with PCA [100] to embed the following data to a 2D space; the visualizations of CEM trajectories are shown in Figure 5 and Figure 6:

- Latent programs from the training dataset encoded by a learned encoder q_ϕ , visualized as blue scatters. There are 35k training programs. This is to visualize the shape of the program distribution in the learned program embedding space. This is also visualized in Figure 4.
- Ground-truth (GT) programs that exhibit optimal behaviors for solving the Karel tasks, visualized as red stars (\star). Ideally, the CEM population should iteratively move toward where the GT programs are located.
- CEM population is a batch of sampled candidate latent programs at each iteration, visualized as red scatters. Each candidate latent program can be decoded as a program that can be executed in the task environment to obtain a reward. By averaging the reward obtained by every candidate latent program, we can calculate the average reward of this population and show it in the figures as Avg. Reward.
- CEM Next Center, visualized as cross signs (\times), indicates the center vector around which the next batch of candidate latent programs will be sampled. This vector is calculated based on a set of candidate latent programs that achieve best reward (*i.e.* elite samples) at each iteration. In this case, it is a weighted average based on the reward each candidate gets from its execution.

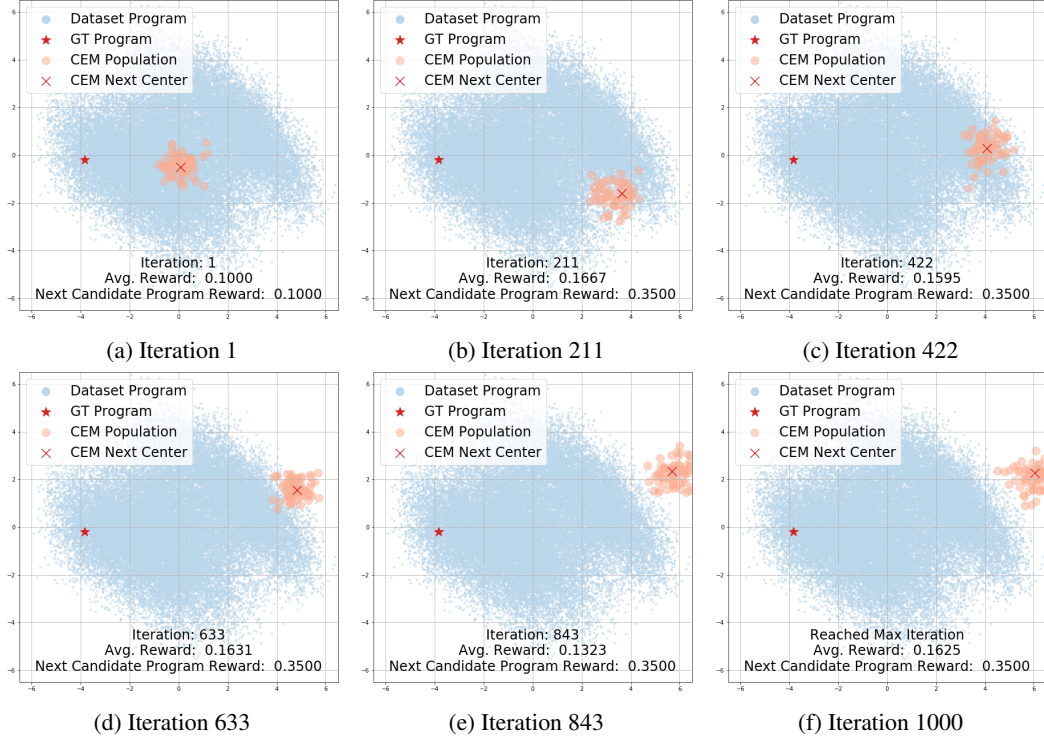


Figure 6: FOURCORNER CEM Trajectory Visualization. Latent training programs from the training dataset, a ground-truth program for the FOURCORNER task, CEM populations, and CEM next candidate programs are embedded to a 2D space using PCA. The CEM trajectory does not converge. The ground-truth program lies far away from the initial sampled distribution, which might contribute to the difficulty of converging.

From Figure 5, we observe that both the average reward of the entire population and the reward of the next candidate program (CEM Next Center) consistently increase as the number of iterations increases, justifying the effectiveness of CEM. Moreover, we observe that the CEM population gradually moves toward where the ground-truth program is located, which aligns well with the fact that our proposed framework can reliably synthesize task-solving programs.

Yet, the populations might not always exactly converge to where the ground-truth latent program is. We hypothesize this could be attributed to the following reasons:

1. CEM convergence: while the CEM search converges, it can still be suboptimal. Since the search terminates when the next candidate latent program obtains the maximum reward (1.1 as shown in the figure) for 10 iterations, it might not exactly converge to where a ground-truth program is.
2. Dimensionality reduction: we visualized the trajectories and programs by performing dimensionality reduction from 256 to 2 dimensions with PCA, which could cause visual distortions.
3. Suboptimal learned program embedding space: while we aim to learn a program embedding space where all the programs inducing the same behaviors are mapped to the same spot in the embedding space, it is still possible that programs that induce the desired behavior can distribute to more than one location in a learned program embedding space. Therefore, CEM search can converge to somewhere that is different from the ground-truth latent program.

On the other hand, the CEM trajectory shown in Figure 6 does not converge and terminates when reaching the maximum number of iterations. The ground-truth program lies far away from the initial sampled distribution, which might contribute to the difficulty of converging. This aligns with the relatively unsatisfactory performance achieved by LEAPS. Employing a more sophisticated searching

Table 5: Decoded linear interpolations of programs close to each other in the latent space.

Latent Program	Decoded Program
START	<code>DEF run m(turnRight move WHILE c(frontIsClear c) w(move w) WHILE c(not c(frontIsClear c) c) w(move w) IF c(frontIsClear c) i(move i) m)</code>
1	<code>DEF run m(turnRight move WHILE c(frontIsClear c) w(move w) WHILE c(not c(frontIsClear c) c) w(move w) IF c(frontIsClear c) i(move i) m)</code>
2	<code>DEF run m(turnRight move WHILE c(frontIsClear c) w(move w) IF c(not c(frontIsClear c) c) i(move i) m)</code>
3	<code>DEF run m(turnRight move WHILE c(frontIsClear c) w(move w) IF c(not c(frontIsClear c) c) i(move i) m)</code>
4	<code>DEF run m(turnRight move WHILE c(frontIsClear c) w(move w) IF c(not c(frontIsClear c) c) i(move i) m)</code>
5	<code>DEF run m(turnRight move WHILE c(frontIsClear c) w(move w) IF c(not c(frontIsClear c) c) i(move i) m)</code>
6	<code>DEF run m(turnRight move WHILE c(frontIsClear c) w(move w) IF c(not c(frontIsClear c) c) i(move i) m)</code>
7	<code>DEF run m(turnRight move turnLeft WHILE c(frontIsClear c) w(move w) IF c(not c(frontIsClear c) c) i(putMarker i) m)</code>
8	<code>DEF run m(turnRight move turnLeft WHILE c(frontIsClear c) w(move w) IF c(not c(frontIsClear c) c) i(putMarker i) m)</code>
END	<code>DEF run m(turnRight move turnLeft WHILE c(frontIsClear c) w(move w) IF c(not c(frontIsClear c) c) i(putMarker i) m)</code>

Table 6: Decoded linear interpolations of programs far from each other in the latent space.

Latent Program	Decoded Program
START	<code>DEF run m(turnRight turnLeft turnLeft move turnRight putMarker move m)</code>
1	<code>DEF run m(turnRight turnLeft turnLeft move turnRight putMarker move m)</code>
2	<code>DEF run m(turnRight turnLeft turnLeft move WHILE c(frontIsClear c) w(putMarker w) turnRight move m)</code>
3	<code>DEF run m(turnRight turnLeft move turnLeft WHILE c(frontIsClear c) w(putMarker w) move m)</code>
4	<code>DEF run m(turnRight turnLeft move WHILE c(frontIsClear c) w(turnLeft w) IF c(not c(frontIsClear c) c) i(move i) m)</code>
5	<code>DEF run m(turnRight move turnLeft WHILE c(frontIsClear c) w(move w) IF c(not c(frontIsClear c) c) i(putMarker i) m)</code>
6	<code>DEF run m(move turnRight turnLeft move WHILE c(frontIsClear c) w(IF c(not c(rightIsClear c) c) i(putMarker i) w) m)</code>
7	<code>DEF run m(move turnRight turnLeft move WHILE c(frontIsClear c) w(IF c(not c(rightIsClear c) c) i(turnLeft i) w) m)</code>
8	<code>DEF run m(move turnRight move WHILE c(frontIsClear c) w(IF c(not c(rightIsClear c) c) i(turnLeft i) w) m)</code>
END	<code>DEF run m(move turnRight move WHILE c(frontIsClear c) w(IF c(not c(rightIsClear c) c) i(turnLeft i) w) m)</code>

algorithm or conducting a more thorough hyperparameter search could potentially improve the performance but it is not the main focus of this work.

C Program Embedding Space Interpolations

To learn a program embedding space that allows for smooth interpolation, we propose three sources of supervision. We aim to verify the effectiveness of it by investigating interpolations in the learned program embedding space. To this end, we follow the procedure described below to produce results shown in Table 5 and Table 6.

1. Sampling a pair of programs from the dataset (START program and END program).
2. Encoding the two programs into the learned program embedding space.
3. Linearly interpolating between the two latent programs to obtain a number of (eight) interpolated latent programs.

Table 7: How predicted programs evolve throughout the course of CEM search for STAIRCLIMBER. See Figure 5 for the corresponding visualization of this CEM search.

Search Iteration	Best Predicted Program
Iteration: 1	<code>DEF run m(IF c(frontIsClear c) i(pickMarker i) WHILE c(leftIsClear c) w(move w) IFELSE c(frontIsClear c) i(turnRight move i) ELSE e(move e) m)</code>
Iteration: 2	<code>DEF run m(WHILE c(markersPresent c) w(move w) IFELSE c(frontIsClear c) i(turnLeft i) ELSE e(move e) WHILE c(leftIsClear c) w(move w) m)</code>
Iteration: 3	<code>DEF run m(WHILE c(not c(frontIsClear c) c) w(move turnRight w) WHILE c(leftIsClear c) w(turnLeft move w) m)</code>
Iteration: 4	<code>DEF run m(WHILE c(not c(frontIsClear c) c) w(pickMarker move w) WHILE c(leftIsClear c) w(turnLeft move w) m)</code>
Iteration: 5	<code>DEF run m(WHILE c(not c(frontIsClear c) c) w(pickMarker turnRight w) WHILE c(leftIsClear c) w(move turnLeft w) m)</code>
Iteration: 6	<code>DEF run m(WHILE c(not c(frontIsClear c) c) w(pickMarker turnRight w) WHILE c(leftIsClear c) w(move turnLeft w) m)</code>
Iteration: 7	<code>DEF run m(WHILE c(not c(leftIsClear c) c) w(turnRight w) IFELSE c(frontIsClear c) i(move i) ELSE e(turnLeft e) WHILE c(rightIsClear c) w(move w) m)</code>
Iteration: 8	<code>DEF run m(WHILE c(not c(leftIsClear c) c) w(turnRight move w) WHILE c(markersPresent c) w(turnLeft move w) m)</code>
Iteration: 9	<code>DEF run m(WHILE c(not c(noMarkersPresent c) c) w(turnRight move w) WHILE c(not c(frontIsClear c) c) w(turnLeft move w) m)</code>
Iteration: 10	<code>DEF run m(WHILE c(not c(noMarkersPresent c) c) w(turnRight move w) WHILE c(leftIsClear c) w(turnLeft move w) m)</code>
Iteration: 11	<code>DEF run m(WHILE c(not c(leftIsClear c) c) w(turnRight move w) WHILE c(noMarkersPresent c) w(turnLeft move w) m)</code>
Iteration: 12	<code>DEF run m(WHILE c(not c(leftIsClear c) c) w(turnRight move w) WHILE c(noMarkersPresent c) w(turnLeft move w) m)</code>
Iteration: 13	<code>DEF run m(WHILE c(not c(leftIsClear c) c) w(turnRight move w) WHILE c(noMarkersPresent c) w(turnLeft move w) m)</code>
Iteration: 14	<code>DEF run m(WHILE c(not c(markersPresent c) c) w(turnRight move w) WHILE c(rightIsClear c) w(move turnLeft w) m)</code>
Iteration: 15	<code>DEF run m(WHILE c(not c(markersPresent c) c) w(turnRight move w) WHILE c(rightIsClear c) w(move turnLeft w) m)</code>
Iteration: 16	<code>DEF run m(WHILE c(not c(markersPresent c) c) w(turnRight move w) WHILE c(rightIsClear c) w(move turnLeft w) m)</code>
Iteration: 17	<code>DEF run m(WHILE c(not c(markersPresent c) c) w(turnRight move w) WHILE c(rightIsClear c) w(move turnLeft w) m)</code>
Iteration: 18	<code>DEF run m(WHILE c(not c(markersPresent c) c) w(turnRight move w) WHILE c(rightIsClear c) w(move turnLeft w) m)</code>
Iteration: 19	<code>DEF run m(WHILE c(not c(markersPresent c) c) w(turnRight move w) WHILE c(rightIsClear c) w(move turnLeft w) m)</code>
Iteration: 20	<code>DEF run m(WHILE c(not c(markersPresent c) c) w(turnRight move w) WHILE c(rightIsClear c) w(move turnLeft w) m)</code>
Iteration: 21	<code>DEF run m(WHILE c(not c(markersPresent c) c) w(turnRight move w) WHILE c(rightIsClear c) w(move turnLeft w) m)</code>
Iteration: 22	<code>DEF run m(WHILE c(not c(markersPresent c) c) w(turnRight move w) WHILE c(rightIsClear c) w(move turnLeft w) m)</code>
Converged	<code>DEF run m(WHILE c(not c(markersPresent c) c) w(turnRight move w) WHILE c(rightIsClear c) w(turnLeft move w) m)</code>

4. Decoding the latent programs to obtain interpolated programs (program 1 to program 8).

We show two pairs of programs and their interpolations in between below as examples. Specifically, the first pair of programs, shown in Table 5, are closer to each other in the latent space and the second pair of programs, shown in Table 6, are further from each other. We observe that the interpolations between the closer program pair exhibit smoother transitions and the interpolations between the further program pair display more dramatic change.

D Program Evolution

In this section, we aim to investigate how predicted programs evolve over the course of searching. We visualize converged CEM search trajectories and the reward each program gets on the StairClimber

Table 8: Mean return (standard deviation) [% increase in performance] after debugging by non-expert humans of LEAPS synthesized programs for 3 statement edits and 5 statement edits. Chosen LEAPS programs are median-reward programs out of 5 LEAPS seeds for each task.

Karel Task	Original Program	3 Edits	5 Edits
TOPOFF	0.86	0.95 (0.07) [10.5%]	1.0 (0.00) [16.3%]
FOURCORNER	0.25	0.75 (0.35) [200%]	0.92 (0.12) [268%]
HARVESTER	0.47	0.85 (0.05) [80.9%]	0.89 (0.00) [89.4%]
Average % Increase	-	97.1%	125%

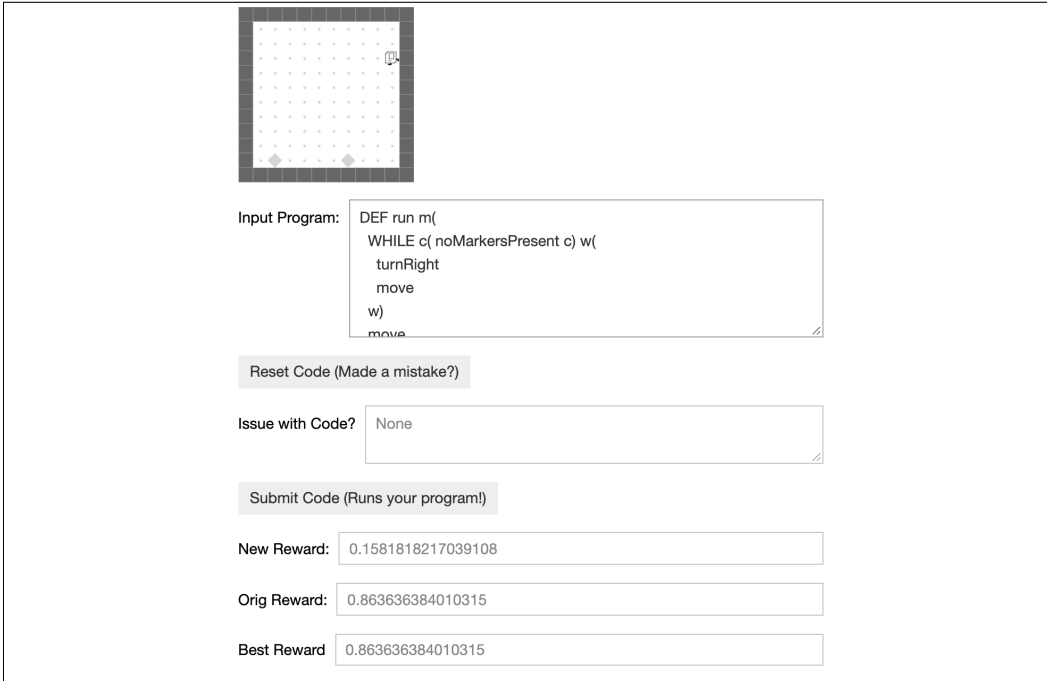


Figure 7: **User Interface for the Human Debugging Interpretability Experiments.** The top contains moving rollout visualizations of the current program in the “Input Program” box, which users are allowed to edit. “Input Program” will first contain the program synthesized by LEAPS. Syntax errors or other issues with code (such as the edit distance being too high) are displayed in the “Issue with Code?” box, the reward of the current inputted program is in the “New Reward” box, and the reward of the original program synthesized by LEAPS is in the “Orig Reward” box. The user’s best reward across all inputted programs is kept track of in the “Best Reward” box.

task in Appendix Figure 5. In Table 7, we present the predicted programs corresponding to the CEM search trajectory on the STAIRCLIMBER task in Figure 5. We observe that the sampled programs consistently improve as the number of iterations increases, justifying the effectiveness of the learned program embedding and the CEM search.

E Interpretability: Human Debugging of LEAPS Programs

Interpretability in Machine Learning is crucial for several reasons [69, 70]. First, *trust* – interpretable machine learning methods and models may more easily be trusted since humans tend to be reluctant to trust systems that they do not understand. Second, interpretability can improve the *safety* of machine learning systems. A machine learning system that is interpretable allows for diagnosing issues (*e.g.* the distribution shift from training data to testing data) earlier and provides more opportunities to intervene. This is especially important for safety-critical tasks such as medical diagnosis [101–105] and real-world robotics [5–11] tasks. Finally, interpretability can lead to *contestability*, by producing

fully debug/test their edited programs. For each program, participants were required to modify up to 5 statements, then attempt the task again with up to only 3 modifications as calculated by the Levenshtein distance metric [106]. A single statement modification is defined as any modification/removal/addition of a IF, WHILE, IFELSE, REPEAT, or ELSE statement, or a removal/addition/change of an action statement (*e.g.* move, turnLeft, etc.). Participants were allowed to ask clarification questions, but we would not answer questions regarding how to specifically improve the performance of their program.

We display example edited programs in Figure 8, and the aggregated results of editing in Table 8. We see a significant increase in performance in all three tasks, with an average 97.1% increase in performance with 3 edits and an average 125% increase in performance with 5. These numbers are averaged over 3 people, with standard deviations reported in the table. Thus we see that even slight modifications to suboptimal LEAPS programs can enable much better Karel task performance when edited by non-expert humans.

Our experiments in this section make an interesting connection to works in program/code repair (*i.e.* automatic bug fixing) [107–120], where the aim is to develop algorithms and models that can find bugs or even repair programs without the intervention of a human programmer. While the goal of these works is to fix programs produced by humans, our goal in this section is to allow humans to improve programs synthesized by the proposed framework.

Another important benefit of programmatic policies is *verifiability* - the ability to verify different properties of policies such as correctness, stability, smoothness, robustness, safety, etc. Since programmatic policies are highly structured, they are more amenable to formal verification methods developed for traditional software systems as compared to neural policies. Recent works [12, 14, 15, 121] show that various properties of programmatic policies (programs written using DSLs, decision trees) can be verified using existing verification algorithms, which can also be applied to programs synthesized by the proposed framework.

<p>WHILE:</p> <pre> DEF run m(WHILE c(frontIsClear c) w(turnRight move pickMarker turnRight w) m) </pre>	<p>IFELSE+WHILE:</p> <pre> DEF run m(IFELSE c(markersPresent c) i(move turnRight i) ELSE e(move e) move move WHILE c(leftIsClear c) w(turnLeft w) m) </pre>	<p>2IF+IFELSE:</p> <pre> DEF run m(IF c(frontIsClear c) i(putMarker i) move IF c(rightIsClear c) i(move i) IFELSE c(frontIsClear c) i(move i) ELSE e(move e) m) </pre>
<p>WHILE+2IF+IFELSE:</p> <pre> DEF run m(WHILE c(leftIsClear c) w(turnLeft w) IF c(frontIsClear c) i(putMarker move i) move IF c(rightIsClear c) i(turnRight move i) IFELSE c(frontIsClear c) i(move i) ELSE e(turnLeft move e) m) </pre>	<p>STAIRCLIMBER:</p> <pre> DEF run m(WHILE c(noMarkersPresent c) w(turnLeft move turnRight move w) m) </pre>	<p>TOPOFF:</p> <pre> DEF run m(WHILE c(frontIsClear c) w(IF c(markersPresent c) i(putMarker i) move w) m) </pre>
<p>CLEANHOUSE:</p> <pre> DEF run m(WHILE c(noMarkersPresent c) w(IF c(leftIsClear c) i(turnLeft i) move IF c(markersPresent c) i(pickMarker i) w) m) </pre>	<p>FOURCORNER:</p> <pre> DEF run m(WHILE c(noMarkersPresent c) w(WHILE c(frontIsClear c) w(move w) IF c(noMarkersPresent c) i((putMarker turnLeft move i) w) m) </pre>	<p>MAZE:</p> <pre> DEF run m(WHILE c(noMarkersPresent c) w(IFELSE c(rightIsClear c) i((turnRight i) ELSE e(WHILE c(not c(frontIsClear c) c) w(turnLeft w) e) move w) m) </pre>
<p>HARVESTER:</p> <pre> DEF run m(WHILE c(markersPresent c) w(WHILE c(markersPresent c) w(pickMarker move w) turnRight move turnLeft WHILE c(markersPresent c) w(pickMarker move w) turnLeft move turnRight w) m) </pre>		

Figure 9: **Ground-Truth Test and Karel Programs.** Here we display ground-truth test set programs used for reconstruction experiments and example ground-truth programs that we write which can solve the Karel tasks (there are an infinite number of programs that can solve each task). Conditionals are enclosed in `c (c)`, while loops are enclosed in `w (w)`, if statements are enclosed in `i (i)`, and the main program is enclosed in `DEF run m(m)`.

F Optimal and Synthesized Programs

In this section, we present the programs from the testing set which are selected for conducting ablation studies in the main paper in Figure 9. Also, we manually write programs that induce optimal behaviors to solve the Karel tasks and present them in Figure 9. Note that while we only show

Naïve

WHILE

```
DEF run m(
  WHILE c(frontIsClear c) w(
    turnRight
    move
    pickMarker
    turnRight
    w)
  m)
```

2IF+IFELSE

```
DEF run m(
  putMarker
  move
  move
  move
  m)
```

IFELSE+WHILE

```
DEF run m(
  move
  move
  move
  turnLeft
  turnLeft
  m)
```

WHILE+2IF+IFELSE

```
DEF run m(
  turnLeft
  putMarker
  move
  move
  WHILE c( markersPresent c) w(
    pickMarker
    pickMarker
    pickMarker
    w)
  m)
```

LEAPS-P

WHILE

```
DEF run m(
  IF c( frontIsClear c) i(
    turnRight
    move
    pickMarker
    turnRight
    i)
  m)
```

2IF+IFELSE

```
DEF run m(
  IFELSE c( not c( frontIsClear c) c) i(
    move
    i) ELSE e(
    putMarker
    move
    e)
  move
  move
  m)
```

IFELSE+WHILE

```
DEF run m(
  IFELSE c( rightIsClear c) i(
    move
    i) ELSE e(
    move
    e)
  move
  move
  IF c( leftIsClear c) i(
    turnLeft
    i)
  m)
```

WHILE+2IF+IFELSE

```
DEF run m(
  WHILE c( leftIsClear c) w(
    turnLeft
    w)
  putMarker
  move
  move
  turnRight
  move
  move
  m)
```

LEAPS-P+R

WHILE

```
DEF run m(
  WHILE c( rightIsClear c) w(
    WHILE c( frontIsClear c) w(
      turnRight
      move
      pickMarker
      turnRight
      w)
    w)
  m)
```

2IF+IFELSE

```
DEF run m(
  IFELSE c( not c( frontIsClear c) c) i(
    move
    i) ELSE e(
    putMarker
    e)
  IFELSE c( rightIsClear c) i(
    move
    i) ELSE e(
    move
    e)
  IF c( rightIsClear c) i(
    move
    i)
  move
  m)
```

IFELSE+WHILE

```
DEF run m(
  REPEAT R=1 r(
    move
    r)
  REPEAT R=2 r(
    move
    r)
  m)
```

WHILE+2IF+IFELSE

```
DEF run m(
  WHILE c( leftIsClear c) w(
    turnLeft
    w)
  putMarker
  move
  move
  turnRight
  move
  move
  m)
```


LEAPS-P+L	
WHILE	IFELSE+WHILE
<pre> DEF run m(WHILE c(frontIsClear c) w(turnRight move pickMarker turnRight w) m) </pre>	<pre> DEF run m(move move move WHILE c(leftIsClear c) w(turnLeft w) m) </pre>
2IF+IFELSE	WHILE+2IF+IFELSE
<pre> DEF run m(IFELSE c(frontIsClear c) i(REPEAT R=0 r(turnRight r) putMarker move i) ELSE e(move e) move move m) </pre>	<pre> DEF run m(WHILE c(leftIsClear c) w(turnLeft w) WHILE c(leftIsClear c) w(turnLeft w) WHILE c(leftIsClear c) w(turnLeft w) IF c(frontIsClear c) i(putMarker move i) move move m) </pre>

LEAPS	
WHILE	IFELSE+WHILE
<pre> DEF run m(WHILE c(frontIsClear c) w(turnRight move pickMarker turnRight w) m) </pre>	<pre> DEF run m(IFELSE c(not c(noMarkersPresent c) c) i(move turnRight i) ELSE e(move e) REPEAT R=2 r(move r) WHILE c(leftIsClear c) w(turnLeft w) m) </pre>
2IF+IFELSE	WHILE+2IF+IFELSE
<pre> DEF run m(IFELSE c(frontIsClear c) i(putMarker move i) ELSE e(move e) IF c(rightIsClear c) i(move i) move m) </pre>	<pre> DEF run m(WHILE c(leftIsClear c) w(turnLeft w) IF c(frontIsClear c) i(putMarker move i) move move m) </pre>

Figure 10: **Example program reconstruction task programs generated by all methods.** The programs that achieve the highest reward while being representative of programs generated by most seeds are shown. The naïve program synthesis baseline usually generates the simplest programs, with fewer conditional statements and loops than the LEAPS ablations. Notably, it fails to generate IFELSE statements on these examples, while LEAPS has no problem doing so.

one optimal program for each task, there exist multiple programs that exhibit the desired behaviors for each task. Then, we analyze the program reconstructed by LEAPS, its ablations, and the naïve program synthesis baseline in Section F.1, and discuss the programs synthesized by LEAPS for Karel tasks in Section F.2.

Table 9: Extended reward comparison on original tasks with 8×8 or 12×12 grids and zero-shot generalization to 100×100 grids. LEAPS achieves the best generalization performance on all the tasks except for HARVESTER.

		STAIRCLIMBER	MAZE	FOURCORNER	TOPOFF	HARVESTER
DRL	Original	1.00 (0.00)	1.00 (0.00)	0.29 (0.05)	0.32 (0.07)	0.90 (0.10)
	100x100	0.00 (0.00)	0.00 (0.00)	0.00 (0.00)	0.01 (0.01)	0.00 (0.00)
DRL-abs	Original	0.13 (0.29)	1.00 (0.00)	0.36 (0.44)	0.63 (0.23)	0.32 (0.18)
	100x100	0.00 (0.00)	0.04 (0.05)	0.37 (0.44)	0.15 (0.12)	0.02 (0.01)
DRL-FCN	Original	1.00 (0.00)	0.97 (0.03)	0.20 (0.34)	0.28 (0.12)	0.46 (0.16)
	100x100	-0.20 (0.10)	0.01 (0.01)	0.00 (0.00)	0.01 (0.01)	0.02 (0.00)
VIPER	Original	0.02 (0.02)	0.69 (0.05)	0.40 (0.42)	0.30 (0.06)	0.51 (0.07)
	100x100	0.00 (0.00)	0.10 (0.12)	0.40 (0.42)	0.03 (0.00)	0.04 (0.00)
LEAPS	Original	1.00 (0.00)	1.00 (0.00)	0.45 (0.40)	0.81 (0.07)	0.45 (0.28)
	100x100	1.00 (0.00)	1.00 (0.00)	0.45 (0.37)	0.21 (0.03)	0.00 (0.00)

synthesis baseline. Those selected programs are shown in Figure 9 and the reconstructed programs are shown in Figure 10.

The naïve program synthesis baseline fails on the complex WHILE+2IF+IFELSE program, as it rarely synthesizes conditional and loop statements, instead generating long sequences of action tokens that attempt to replicate the desired behavior of those statements. We believe that this is because it is incentivized to initially predict action tokens to gain more immediate reward, making it less likely to synthesize other tokens. LEAPS and its variations perform better and synthesize more complex programs, demonstrating the importance of the proposed two-stage learning scheme in biasing program search. Also, LEAPS synthesizes programs that are more concise and induce behaviors which are more similar to given testing programs, justifying the effectiveness of the proposed learning objectives.

F.2 Karel Environment Tasks

This section is complementary to the main experiments in the main paper, where we compare LEAPS against the baselines on a set of Karel tasks, which is described in detail in Section K. The programs synthesized by LEAPS are presented in Figure 11.

The synthesized programs solve both STAIRCLIMBER and MAZE. For TOPOFF, since the average expected number of markers presented in the last row is 3, LEAPS synthesizes a sub-optimal program that conducts the toff behavior three times. For CLEANHOUSE, while all the baselines fail on this task, the synthesized program achieves some performance by simply moving around and try to pick up markers. For HARVESTER, LEAPS fails to acquire the desired behavior that required nested loops but produces a sub-optimal program that contains only action tokens.

G Additional Generalization Experiments

Here, we present additional generalization experiments to complement those presented in Section 5.6. In Section G.1, we extend the 100x100 state size zero-shot generalization experiments to 3 additional tasks. In Section G.2, we analyze how well baseline methods and LEAPS can generalize to unseen configurations of a given task.

G.1 Generalization on FOURCORNER, TOPOFF, and HARVESTER

Evaluating zero-shot generalization performance assumes methods to work reasonably well on the original tasks. For this reason (and due to space limitations) we present only STAIRCLIMBER and MAZE for generalization experiments in the main text in Section 5.6 because most methods achieve reasonable performance on these two tasks, with DRL and LEAPS both solving these tasks fully and DRL-abs solving Maze fully.

However, here we also present full results for all tasks except CLEANHOUSE (as no method except LEAPS has a reasonable level of performance on it). The results are summarized in Table 9. We see that LEAPS generalizes well on FOURCORNER and maintains the best performance on TOPOFF. It is outperformed on HARVESTER, although none of the methods do well on HARVESTER as the highest

Table 10: Mean return (standard deviation) [% change in performance] on generalizing to unseen configurations on TOPOFF and HARVESTER task.

TOPOFF	Training configuration %				
	75%	50%	25%	10%	5%
DRL	0.17 (0.05) [-46.8%]	0.12 (0.09) [-62.5%]	0.12 (0.06) [-62.5%]	0.17 (0.13) [-46.8%]	0.13 (0.04) [-59.4%]
DRL-abs	0.23 (0.29) [-63.5%]	0.29 (0.36) [-54.0%]	0.45 (0.45) [-28.6%]	0.24 (0.38) [-61.9%]	0.26 (0.37) [-18.8%]
VIPER	0.27 (0.03) [-10.0%]	0.28 (0.04) [-6.67%]	0.27 (0.06) [-10.0%]	0.27 (0.02) [-10.0%]	0.28 (0.03) [-6.67%]
LEAPS	0.68 (0.18) [-15.0%]	0.65 (0.13) [-18.8%]	0.61 (0.24) [-23.8%]	0.68 (0.21) [-15.0%]	0.67 (0.18) [-16.3%]

HARVESTER	Training configuration %				
	75%	50%	25%	10%	5%
DRL	0.64 (0.24) [-28.9%]	0.71 (0.29) [-21.1%]	0.21 (0.06) [-76.7%]	0.14 (0.09) [-84.4%]	0.04 (0.01) [-95.6%]
DRL-abs	0.14 (0.21) [-56.3%]	0.24 (0.25) [-25.0%]	0.05 (0.06) [-84.4%]	0.13 (0.21) [-59.4%]	0.31 (0.31) [-3.13%]
VIPER	0.54 (0.01) [+5.88%]	0.54 (0.02) [+5.88%]	0.55 (0.01) [+7.84%]	0.54 (0.01) [+5.88%]	0.44 (0.22) [-13.7%]
LEAPS	0.40 (0.30) [-13.0%]	0.42 (0.27) [-8.69%]	0.50 (0.35) [+08.69%]	0.12 (0.19) [-73.9%]	0.01 (0.03) [-97.6%]

obtained reward by any method is 0.04 (by VIPER). In summary, LEAPS performs the best on 4 out of these 5 tasks, further demonstrating its superior zero-shot generalization performance.

Furthermore, we note that it is possible that a DRL policy employing a fully convolutional network (FCN) as proposed in Long et al. [122] can handle varying observation sizes. FCNs were also demonstrated in Silver et al. [49] to demonstrate better generalization performance than traditional convolutional neural network policies. However, we hypothesize that the generalization performance here will still be poor as there is a large increase in the number of features that the FCN architecture needs to aggregate when transferring from $8 \times 8 / 12 \times 12$ state inputs to 100×100 inputs—a 10x input size increase that FCN is not specifically designed to deal with. We have included both FCN’s zero-shot generalization results and its results on the original grid sizes in Table 9. DRL-FCN, where we have replaced the policy and value function networks of PPO with an FCN, does manage to perform zero-shot transfer marginally better than DRL performs when training from scratch (as it DRL’s architecture cannot handle varied input sizes) on MAZE and HARVESTER. However, it obtains a negative reward on STAIRCLIMBER as it attempts to navigate away from the stairs when transferring to the 100×100 grid size. Its performance is still far worse than LEAPS and VIPER on most tasks, demonstrating that the programmatic structure of the policy is important for these tasks.

G.2 Generalization to Unseen Configurations

We present a generalization experiment in the main paper to study how well the baselines and the programs synthesized by the proposed framework can generalize to larger state spaces that are unseen during training without further learning on the STAIRCLIMBER and MAZE tasks. In this section, we investigate the ability of generalizing to different configurations, which are defined based on the marker placement related to solve a task, on both the TOPOFF task and HARVESTER task.

Since solving TOPOFF requires an agent to put markers on top of all markers on the last row, the initial configurations are determined by the marker presence on the last row. The grid has a size of 10×10 inside the surrounding wall. We do not spawn a marker at the bottom right corner in the last row, leaving 9 possible locations with marker, allowing 2^9 possible initial configurations. On the other hand, HARVESTER requires an agent to pick up all the markers placed in the grid. The grid has a size of 6×6 inside the surrounding wall, leaving 36 possible locations in grid with a marker, resulting in 2^{36} possible initial configurations.

We aim to test if methods can learn from only a small portion of configurations during training and still generalize to all the possible configurations without further learning. To this end, we experiment using 75%, 50%, 25%, 10%, 5% of the configurations for training DRL, DRL-abs, and VIPER and for the program search stage of LEAPS. Then, we test zero-shot generalization of the learned models and programs on all the possible configurations. We report the performance in Table 10. We compare the performance each method achieves to its own performance learning from all the configurations (reported in the main paper) to investigate how limiting training configurations affects the performance. Note that the results of training and testing on 100% configurations are reported in the main paper, where no generalization is required.

TOPOFF. LEAPS outperforms all the baselines on the mean return on all the experiments. VIPER and LEAPS enjoy the lowest and the second lowest performance decrease when learning from only a portion of configurations, which demonstrates the strength of programmatic policies. DRL-abs slightly outperforms DRL, with better absolute performance and lower performance decrease. We believe that this is because DRL takes entire Karel grids as input, and therefore held out configurations are completely unseen to it. In contrast, DRL-abs takes abstract states (*i.e.* local perceptions) as input, which can alleviate this issue.

HARVESTER. VIPER outperforms almost all other methods on absolute performance and performance decrease, while LEAPS achieves second best results, which again justifies the generalization of programmatic policies. Both DRL and DRL-abs are unable to generalize well when learning from a limited set of configurations, except in the case of DRL-abs learning from 5% of configurations, which can be attributed to the high-variance of DRL-abs results.

H Additional Analysis on Experimental Results

Due to the limited space in the main paper, we include additional analysis of the experimental results in this section.

H.1 DRL vs. DRL-abs

We hypothesize that DRL-abs does not always outperform DRL due to imperfect perception (*i.e.* state abstraction) design. DRL-abs takes abstract states as input (*i.e.* `frontIsClear()`, `leftIsClear()`, `rightIsClear()`, `markerPresent()` in our design), which only describe local perception while omitting the information of the entire map. Therefore, for tasks such as STAIRCLIMBER, HARVESTER, and CLEANHOUSE, which would be easier to solve with access to the entire Karel grid, DRL might outperform DRL-abs. In this work, DRL-abs’ abstract states are the perceptions from the DSL we synthesize programs with to make the comparisons fair against our method as well as analyzing the effects of abstract states in the DRL domain. However, a more sophisticated design for perception/state abstraction could potentially improve the performance of DRL-abs.

H.2 VIPER generalization

VIPER operates on the abstract state space which is invariant to grid size. However, for the reasons below, it is still unable to transfer the behavior to the larger grid despite its abstract state representation. We hypothesize that VIPER’s performance suffers on zero-shot generalization for two main reasons.

1. It is constrained to imitate the DRL teacher policy during training, which is trained on the smaller grid sizes. Thus its learned policy also experiences difficulty in zero-shot generalization to larger grid sizes.
2. Its decision tree policies cannot represent certain looping behaviors as they simply perform a one-to-one mapping from abstract state to action, thus making it difficult to learn optimal behaviors that require a one-to-many mapping between an abstract state and a set of desired actions. Empirically, we observed that training losses for VIPER decision trees were much higher for tasks such as STAIRCLIMBER which require such behaviors.

I Detailed Descriptions and Illustrations of Ablations and Baselines

This section provides details on the variations of LEAPS used for ablations studies and the baselines which we compare against. The descriptions of the ablations of LEAPS are presented in Section I.1 and the illustrations are shown in Figure 12. The naïve program synthesis baseline is illustrated in Figure 13 (c) for better visualization. Then, the descriptions of the baselines are presented in Section I.2 and the illustrations are shown in Figure 13.

I.1 Ablations

We first ablate various components of our proposed framework in order to (1) justify the necessity of the proposed two-stage learning scheme and (2) identify the effects of the proposed objectives. We consider the following baselines and ablations of our method.

- Naïve: the naïve program synthesis baseline is a policy that learns to directly synthesize a program from scratch by recurrently predicting a sequence of program tokens. The architecture of this baseline is a recurrent neural network which takes an initial starting token as the input at the first time step, and then sequentially outputs a program token at each time step to compose a program until an end token is produced. Note that the observation of this baseline is its own previously outputted program token instead of the state of the task environment (*e.g.* Karel grids). Also, at each time step, this baseline produces a distribution over all the possible program tokens in the given DSL instead of a distribution over agent’s action in the task environment (*e.g.* `move()`). This baseline investigates if an end-to-end learning method can solve the problem. This baseline is illustrated in Figure 13 (c).
- LEAPS-P: the simplest ablation of LEAPS, in which the program embedding space is learned by only optimizing the program reconstruction loss \mathcal{L}^P . This baseline is illustrated in Figure 12 (a).
- LEAPS-P+R: an ablation of LEAPS which optimizes both the program reconstruction loss \mathcal{L}^P and the program behavior reconstruction loss \mathcal{L}^R . This baseline is illustrated in Figure 12 (b).
- LEAPS-P+L: an ablation of LEAPS which optimizes both the program reconstruction loss \mathcal{L}^P and the latent behavior reconstruction loss \mathcal{L}^L . This baseline is illustrated in Figure 12 (c).
- LEAPS (LEAPS-P+R+L): LEAPS with all the losses, optimizing our full objective.
- LEAPS-rand- $\{8/64\}$: like LEAPS, this ablation also optimizes the full objective for learning the program embedding space. But when searching latent programs, instead of CEM, it simply randomly samples 8/64 candidate latent programs and chooses the best performing one. These baselines justify the effectiveness of using CEM for searching latent programs.

I.2 Baselines

We evaluate LEAPS against the following baselines (illustrated in Figure 13).

- DRL: a neural network policy trained on each task and taking raw states (Karel grids) as input. A Karel grid is represented as a binary tensor with dimension $W \times H \times 16$ (there are 16 possible states for each grid square) instead of an image. This baseline is illustrated in Figure 13 (a).
- DRL-abs: a recurrent neural network policy directly trained on each Karel task but instead of taking raw states (Karel grids) as input it takes *abstract* states as input (*i.e.* it sees the same perceptions as LEAPS). Specifically, all returned values of perceptions including `frontIsClear()==true`, `leftIsClear()==false`, `rightIsClear()==true`, `markersPresent()==false`, and `noMarkersPresent()==true` are concatenated as a binary vector, which is then fed to the DRL-abs policy as its input. This baseline allows for a fair comparison to LEAPS since the program execution process also utilizes abstract state information. This baseline is illustrated in Figure 13 (b).
- DRL-abs-t: a DRL *transfer* learning baseline in which for each task, we train DRL-abs policies on all other tasks, then fine-tune them on the current task. Thus it acquires a prior by learning to first solve other Karel tasks. Rewards are reported for the policies from the task that transferred with highest return. We only transfer DRL-abs policies as some tasks have different state spaces so that transferring a DRL policy trained on a task to another task with a different state space is not possible.
This baseline is designed to investigate if acquiring task related priors allows DRL policies to perform better on our Karel tasks. Unlike LEAPS, which acquires priors from a dataset consisting of randomly generated programs and the behaviors those program induce in the environment, DRL-abs-t allows for acquiring priors from goal-oriented behaviors (*i.e.* other Karel tasks).
- HRL: a hierarchical RL baseline in which a VAE is first trained on action sequences from program execution traces used by LEAPS. Once trained, the decoder is utilized as a low-level policy for

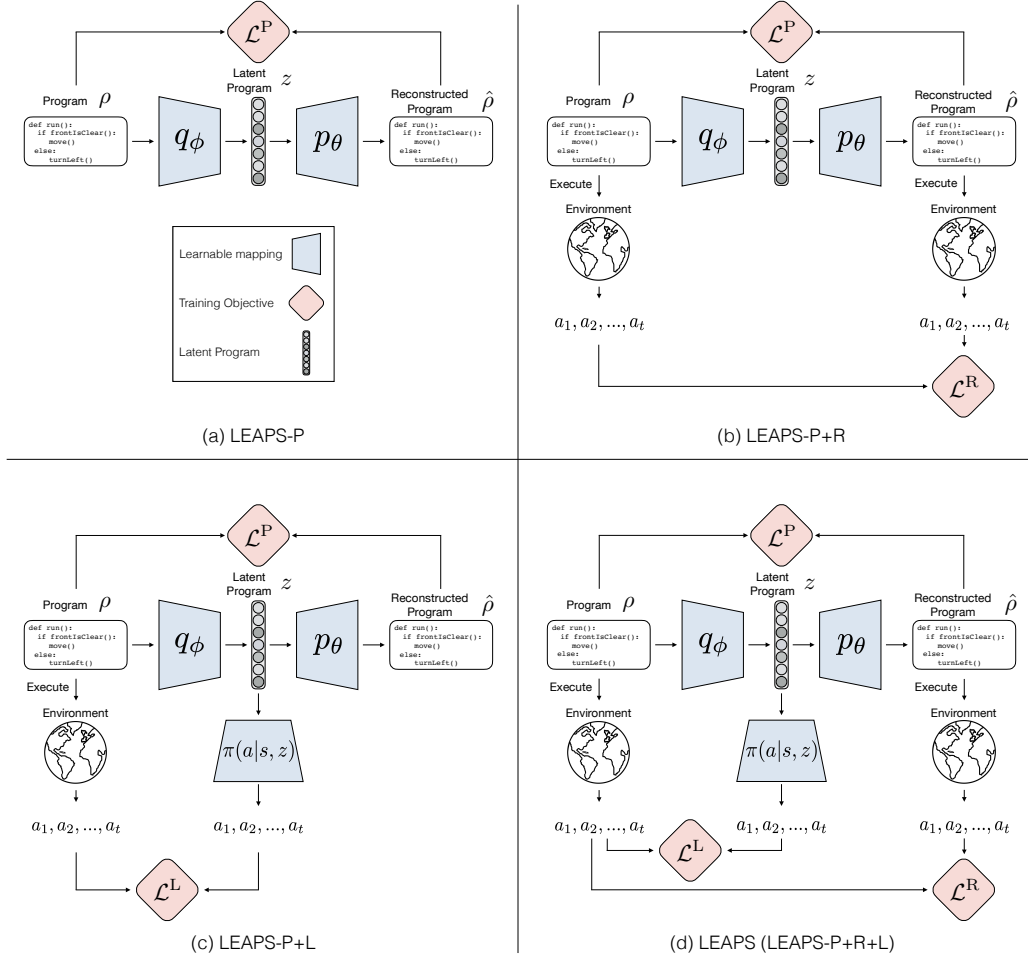


Figure 12: **LEAPS Variations Illustrations.** Blue trapezoids represent the modules whose parameters are being learned in the learning program embedding stage. Red diamonds represent the learning objectives. Gray rounded rectangle represent latent programs (*i.e.* program embeddings), which are vectors. (a) LEAPS-P: the simplest ablation of LEAPS, in which the program embedding space is learned by only optimizing the program reconstruction loss \mathcal{L}^P . (b) LEAPS-P+R: an ablation of LEAPS which optimizes both the program reconstruction loss \mathcal{L}^P and the program behavior reconstruction loss \mathcal{L}^R . (c) LEAPS-P+L: an ablation of LEAPS which optimizes both the program reconstruction loss \mathcal{L}^P and the latent behavior reconstruction loss \mathcal{L}^L . (d) LEAPS (LEAPS-P+R+L): our proposed framework that optimizes all the proposed objectives.

learning a high-level policy to sample actions from. Similar to LEAPS, this baseline utilizes the dataset to produce a prior of the domain. It takes raw states (Karel grids) as input.

This baseline is also designed to investigate if acquiring priors allow DRL policies to perform better. Similar to LEAPS, which acquires priors from a dataset consisting of randomly generated programs and the behaviors those program induce in the environment, HRL is trained to acquire priors by learning to reconstruct the behaviors induced by the programs. One can also view this baseline as a version of the framework proposed in [123] with some simplifications, which also learns an embedding space using a VAE and then trains a high-level policy to utilize this embedding space together with the low-level policy whose parameters are frozen. This baseline is illustrated in Figure 13 (d).

- HRL-abs: the same method as HRL but taking abstract states (*i.e.* local perceptions) as input. This baseline is illustrated in Figure 13 (d).

- VIPER [12]: A decision-tree programmatic policy which imitates the behavior of a deep RL teacher policy via a modified DAgger algorithm [66]. This decision tree policy cannot synthesize loops, allowing us to highlight the performance advantages of more expressive program representation that LEAPS is able to take advantage of.

All the baselines are trained with PPO [67] or SAC [68], including the VIPER teacher policy. More training details can be found in Section L.

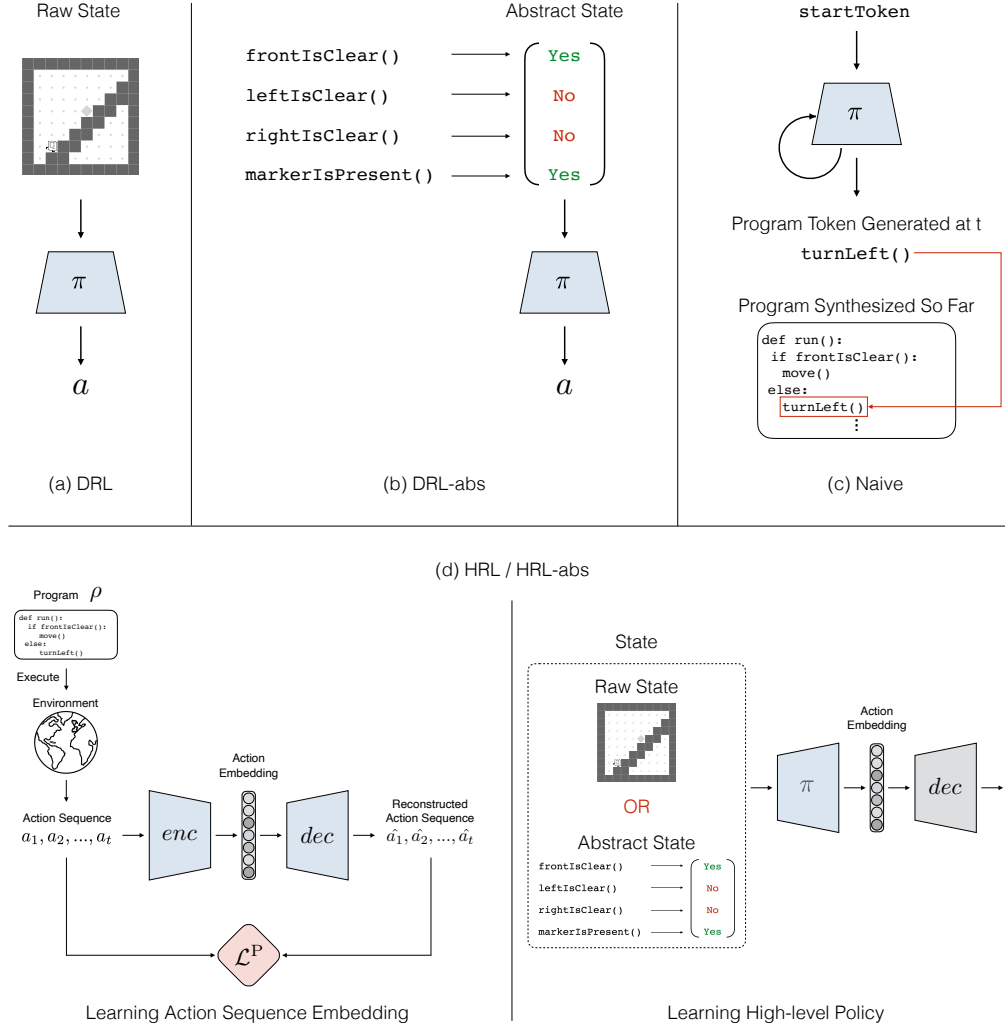


Figure 13: **Baseline Methods Illustrations.** (a) DRL: a DRL policy that takes raw state input (*i.e.* a Karel grid represented as a $W \times H \times 12$ binary tensor as there are 12 possible states for each grid square). (b) DRL-abs: a DRL policy that takes abstract state input, containing a vector of returned values of perceptions, *e.g.* `frontIsClear() == true` and `markersPresent() == false`. (c) Naive: a naïve program synthesis baseline that learns to directly synthesize a program from scratch by recurrently predicting a sequence of program tokens. (d) HRL/HRL-abs: a hierarchical RL baseline in which a VAE, consisting of an encoder *enc* and a decoder *dec*, is first trained to reconstruct action sequences from program execution traces used by LEAPS. Once the action embedding space is learned, it employs a high-level policy π that learns from scratch to solve task by predicting a distribution in the learned action embedding space. Note that the parameters of the decoder *dec* are frozen (represented in gray) when the high-level policy is learning. The HRL policy takes raw state input (same as the DRL baseline) and the HRL-abs policy takes abstract state input (same as the DRL-abs baseline).

J Program Dataset Generation Details

To learn a program embedding space for the proposed framework and its ablations, we randomly generate 50k programs to form a dataset with 35k training programs and 7.5k programs for validation and testing. Simply generating programs by uniformly sampling all the tokens from the DSL would yield programs that mainly only contain action tokens since the chance to synthesize conditional statements with correct grammar is low. Therefore, to produce programs that are longer and deeply nested with conditional statements to induce more complex behaviors, we propose to sample programs using a probabilistic sampler.

To generate each program, we sample program tokens according to the probabilities listed in Table 11 at every step until we sample an ending token or when a maximum program length is reached. When generating programs, we ensure that no program is identical to any other. Each token is generated sequentially, and length is effectively governed by the `STMT_STMT` token detailed in Table 11’s caption. There is a maximum depth limit of 4 nested conditional/loop statements, and a maximum statement depth limit of 6 (can’t have more than 6 nested `STMT_STMT` tokens). Note that this sampling procedure does not guarantee that the programs generated will terminate, hence when executing them to obtain ground-truth interactions for training the Program Behavior and Latent Behavior Reconstruction losses we limit the max program execution length to 100 environment timesteps. This sampling procedure results in the distribution of program lengths seen in Figure 14.

Intuitively, shorter lengths can bias synthesized programs to compress the same behaviors into fewer tokens through the use of loops, making program search easier. Therefore, in our experiments, we have limited the maximum output program length of LEAPS to 45 tokens (as the maximum in the dataset is 44). As shown in the example programs generated by LEAPS in Figure 11, LEAPS successfully generates loops for our Karel tasks, which can be probably attributed to this bias of program length. We further verify this intuition by rerunning LEAPS with the max program length set to 100 tokens on the Karel tasks. We display generated programs in Table 12, where we see that some of the generated programs are indeed much longer and lack loop statements and structures.

Table 11: The probability of sampling program tokens when generating the program dataset. Tokens are generated sequentially, and `STMT_STMT` refers to breaking up the current token into two tokens, each of which is selected according to the same probability distribution again. Thus it effectively controls how long programs will be.

	WHILE	REPEAT	STMT_STMT	ACTION	IF	IFELSE
Standard Dataset	0.15	0.03	0.5	0.2	0.08	0.04

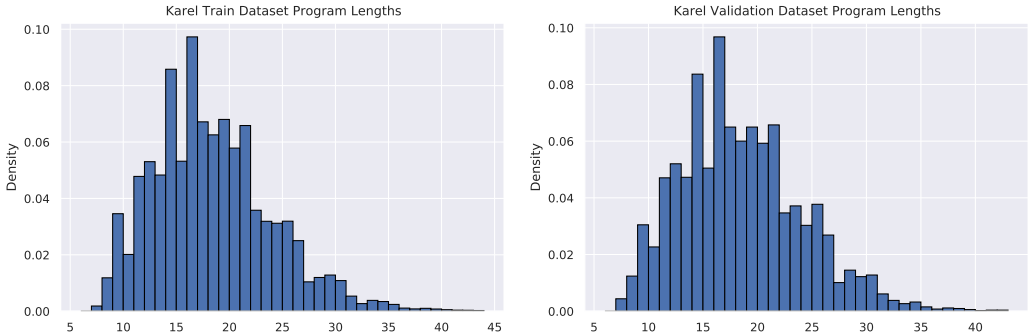


Figure 14: Histograms of the program length (*i.e.* number of program tokens) in the training and validation datasets.

K Karel Task Details

MDP Tasks We utilize environment state based reward functions for the RL tasks `STAIRCLIMBER`, `FOURCORNER`, `TOPOFF`, `MAZE`, `HARVESTER`, and `CLEANHOUSE`. For each task, we average

Table 12: **LEAPS Length 100 Synthesized Karel Programs.** Line breaks are not shown here as the programs are very long. The examples picked are ones that represent the programs generated by most seeds for each task. Without the 45 token restriction on program lengths, programs for TOPOFF, FOURCORNER, and HARVESTER are very long and have repetitive movements that can easily be put into REPEAT or WHILE loops. The CLEANHOUSE program also contains repeated, somewhat redundant WHILE loops. MAZE and STAIRCLIMBER programs are mostly unaffected by the change in maximum program length. These programs demonstrate that the bias induced by program length restriction is important for producing more complex programs in the program synthesis phase of LEAPS.

Karel Task	Program
STAIRCLIMBER	<pre>DEF run m(turnLeft turnRight turnLeft turnLeft turnRight WHILE c(noMarkersPresent c)) w(turnLeft move w) m)</pre>
TOPOFF	<pre>DEF run m(WHILE c(noMarkersPresent c) w(move w) turnRight turnRight turnRight turnRight turnRight) turnRight turnRight turnRight turnRight turnRight turnRight turnRight turnRight turnRight turnRight turnRight turnRight turnRight turnRight turnRight turnRight putMarker turnRight turnRight move turnRight move turnRight move turnRight move turnRight move turnRight move turnRight move turnRight move turnRight move turnRight move turnRight move turnRight move turnRight move turnRight move turnRight move turnRight move turnRight move turnRight move turnRight move m)</pre>
CLEANHOUSE	<pre>DEF run m(turnRight pickMarker turnLeft turnRight turnLeft pickMarker move turnLeft WHILE c(leftIsClear c) w(pickMarker move w) turnRight turnLeft pickMarker move turnLeft WHILE c(leftIsClear c) w(pickMarker move w) turnLeft pickMarker) WHILE c(leftIsClear c) w(pickMarker move turnLeft pickMarker w) } WHILE c(noMarkersPresent c) w(turnLeft move pickMarker w) turnLeft pickMarker turnLeft m)</pre>
FOURCORNER	<pre>DEF run m(turnRight WHILE c(frontIsClear c) w(move w) turnRight WHILE c(frontIsClear c) w(move w) turnRight WHILE c(frontIsClear c) w(move w) turnRight putMarker WHILE c(frontIsClear c) w(move w) turnRight putMarker WHILE c(frontIsClear c) w(move w) } turnRight putMarker WHILE c(frontIsClear c) w(move w) turnRight putMarker m)</pre>
MAZE	<pre>DEF run m(WHILE c(noMarkersPresent c) w(REPEAT R=1 r(turnRight r) move w) turnLeft turnRight m)</pre>
HARVESTER	<pre>DEF run m(turnLeft turnRight pickMarker move pickMarker move turnRight move pickMarker move pickMarker move turnRight move pickMarker move pickMarker move pickMarker move turnRight move pickMarker move pickMarker move pickMarker move pickMarker move turnRight move pickMarker move pickMarker move pickMarker move pickMarker move pickMarker move pickMarker move pickMarker move pickMarker move pickMarker move pickMarker move pickMarker move pickMarker move pickMarker move pickMarker move turnRight move pickMarker move pickMarker move pickMarker move pickMarker move pickMarker move pickMarker move pickMarker move pickMarker move pickMarker move pickMarker move turnRight move m)</pre>

performance of the policies on 10 random environment start configurations. For all tasks with marker placing objectives, the final reward will be 0—regardless of the any other agent actions—if a marker is placed in the wrong location. This is done in order to discourage “spamming” marker placement on every grid location to exploit the reward functions. All rewards described below are then normalized so that the return is between $[0, 1.0]$ for tasks without penalties, and $[-1.0, 1.0]$ for tasks with negative penalties, for easier learning for the DRL methods. We visualize all tasks as well as their start and ideal end states in Figure 15 on a 10×10 grid for consistency in the visualizations (except CLEANHOUSE).

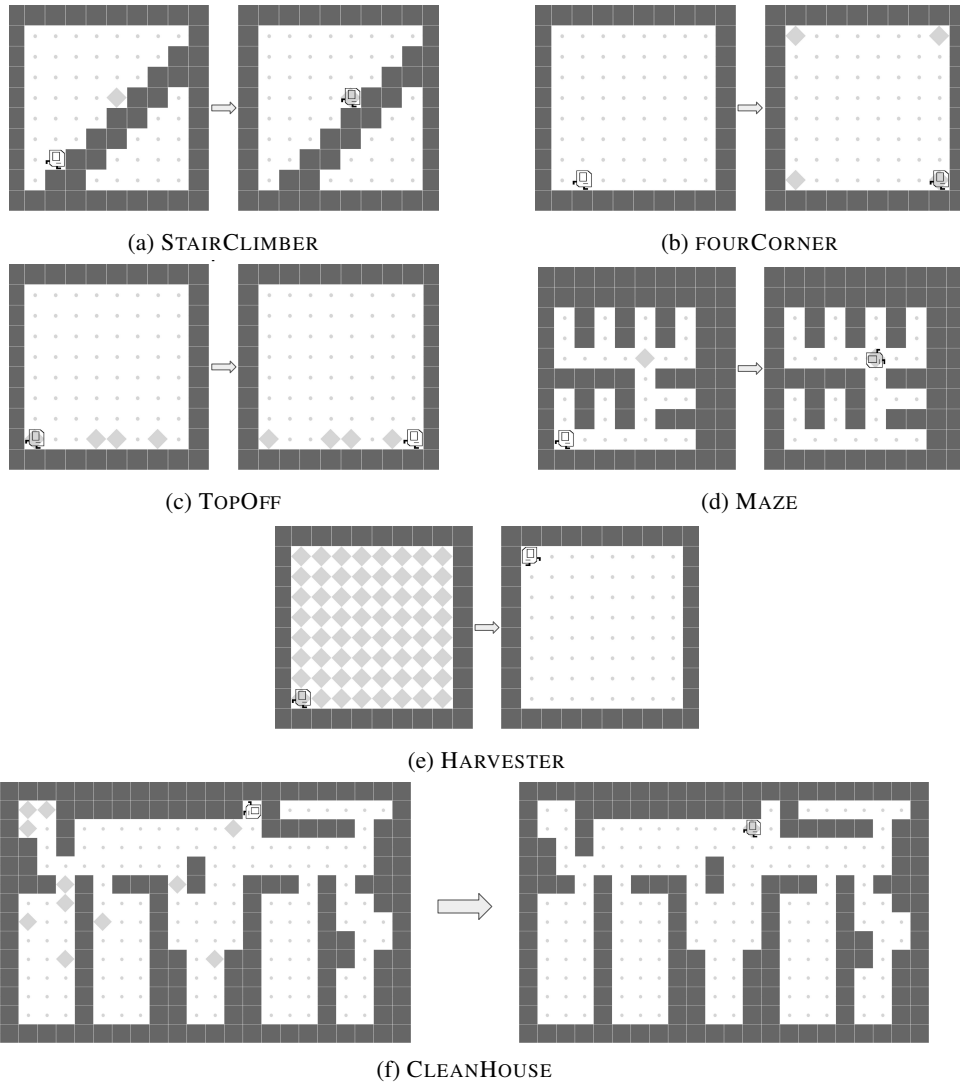


Figure 15: Example of initial configurations and their ideal end states of the Karel tasks. Note that we show only one example of initial configuration and its ideal end state pair for each task. However, markers, walls and agent’s position are randomized in initial configurations depending upon task. Please see section K for more details.

K.1 STAIRCLIMBER

The goal is to climb the stairs to reach where the marker is located. The reward is defined as a sparse reward: 1 if the agent reaches the goal in the environment rollout, -1 if the agent moves to a position off of the stairs during the rollout, and 0 otherwise. This is on a 12×12 grid, and the marker location and agent’s initial location are randomized between rollouts.

K.2 FOURCORNER

The goal is to place a marker at each corner of the Karel environment grid. The reward is defined as sum of corners having a marker divided by four. If the Karel state has a marker placed in wrong location, the reward will be 0. This is on a 12×12 grid.

K.3 TOPOFF

The goal is to place a marker wherever there is already a marker in the last row of the environment, and end up in the rightmost square on the bottom row at the end of the rollout. The reward is defined as the number of consecutive places until the agent either forgets to place a marker where the marker is already present or places a marker at an empty location in last row, with a bonus for ending up on the last square. This is on a 12×12 grid, and the marker locations in the last row are randomized between rollouts.

K.4 MAZE

The goal is to find a marker in randomly generated maze. The reward is defined as a sparse reward: 1 if the agent finds the marker in the environment rollout, 0 otherwise. This is on a 8×8 grid, and the marker location, agent’s initial location, and the maze configuration itself are randomized between rollouts.

K.5 CLEANHOUSE

We design a complex 14×22 Karel environment grid that resembles an apartment. The goal is to pick up the garbage (markers) placed at 10 different locations and reach the location where there is a dustbin (2 markers in 1 location). To make the task simpler, we place the markers adjacent to any wall in the environment. The reward is defined as total locations cleaned (markers picked) out of the total number of markers placed in initial Karel environment state (10). The agent’s initial location is fixed but the marker locations are randomized between rollouts.

K.6 HARVESTER

The goal is to pickup a marker from each location in the Karel environment. The final reward is defined as the number of markers picked up divided the total markers present in the initial Karel environment state. This is on a 8×8 grid. We run both MAZE and HARVESTER on smaller Karel environment grids to save time and compute resources because these are long horizon tasks.

L Hyperparameters and Training Details

L.1 DRL and DRL-abs

RL training directly on the Karel environment is performed with the PPO algorithm [67] for 2M timesteps using the ALF codebase⁴. We tried a discretized SAC [68] implementation (by replacing Gaussian distributions with Categorical distributions), but it was outperformed by PPO on the Karel tasks on all environments. We also tried tabular Q-learning from raw Karel grids (it wouldn’t work well on abstract states as the state is partially observed), however it was also consistently outperformed by PPO. For DRL, the policies and value networks are the same with a shared convolutional encoder that first processes the state (as the Karel state size is $(H \times W \times 16)$ for 16 possible agent direction or marker placement values that each state in the grid can take on at a time. The convolutional encoder consists of two layers: the first with 32 filters, kernel size 2, and stride 1, the second with 32 filters, kernel size 4, and stride 1. For DRL-abs, the policy and value networks are both comprised of an LSTM layer and a 2-layer fully connected network, all with hidden sizes of 100.

For each task, we perform a comprehensive hyperparameter grid search over the following parameters, and report results from the run with the best averaged final reward over 5 seeds.

The hyperparameter grid is listed below, shared parameters are also listed:

⁴<https://github.com/HorizonRobotics/alf/>

- Importance Ratio Clipping: {0.05, 0.1, 0.2}
- Advantage Normalization: {True, False}
- Entropy Regularization: {0.1, 0.01, 0.001}
- Number of updates per training iteration (This controls the ratio of gradient steps to environment steps): {1, 4, 8, 16}
- Number of environment steps per set of training iterations: 32
- Number of parallel actors: 10
- Optimizer: Adam
- Learning Rate: 0.001
- Batch Size: 128

Hyperparameters that performed best for each task are listed below.

DRL	Import Ratio Clip	Adv Norm	Entropy Reg	Updates per Train Iter
CLEANHOUSE	0.1	True	0.01	4
FOURCORNER	0.2	True	0.01	16
HARVESTER	0.05	True	0.01	8
MAZE:	0.05	True	0.001	8
STAIRCLIMBER	0.1	True	0.1	4
TOPOFF	0.05	True	0.001	4

DRL-abs	Import Ratio Clip	Adv Norm	Entropy Reg	Updates per Train Iter
CLEANHOUSE	0.2	True	0.01	8
FOURCORNER	0.05	True	0.01	4
HARVESTER	0.2	True	0.01	4
MAZE:	0.2	True	0.001	4
STAIRCLIMBER	0.05	True	0.1	16
TOPOFF	0.2	True	0.001	8

L.2 DRL-abs-t

DRL-abs-t is limited to DRL-abs policies as the state spaces are different for some of the Karel tasks. For DRL-abs-t, we use the best hyperparameter configuration for each Karel task to train a policy to 1M timesteps. Then, we attempt direct policy transfer to each other task by training for another 1M timesteps on the new task with the same hyperparameters (excluding transferring to the same task). Numbers reported are from the task transfer that achieved the highest reward. The tasks that we transfer from for each task are listed below:

DRL-abs-t	Transferred from
CLEANHOUSE	HARVESTER
FOURCORNER	TOPOFF
HARVESTER	MAZE
MAZE	STAIRCLIMBER
STAIRCLIMBER	HARVESTER
TOPOFF	HARVESTER

L.3 HRL

Pretraining stage: We first train a VAE to reconstruct action trajectories generated from our program dataset. For each program, we generate 10 rollouts in randomly configured Karel environments to produce the HRL dataset, giving this baseline the same data as LEAPS. These variable-length action

sequences are encoded via an LSTM encoder into a 10-dimensional, continuous latent space and decoded by an LSTM decoder into the original action trajectories. We chose 10-dimensional so as to not make downstream RL too difficult. We tune the KL divergence weight (β) of this network such that it’s as high as possible while being able to reconstruct the trajectories well. Network/training details below:

- β : 1.0
- Optimizer: Adam (All optimizers)
- Learning Rates: 0.0003
- Hidden layer size: 128
- # LSTM layers (both encoder/decoder): 2
- Latent embedding size: 10
- Nonlinearity: ReLU
- Batch Size: 128

Downstream (Hierarchical) RL On our Karel tasks, we use the VAE’s decoder to decode latent vectors (actions for the RL agent) into varied-length action sequences for all Karel tasks. The decoder parameters are frozen and used for all environments. The RL agent is retrained from scratch for each task, in the same manner as the standard RL baselines DRL-abs and DRL. We use Soft-Actor Critic (SAC, Haarnoja et al. [68]) as the RL algorithm as it is state of the art in many continuous action space environments. SAC grid search parameters for all environments follow below:

- Number of updates per training iteration: {1, 8}
- Number of environment steps per set of training iterations: 8 (multiplied by the number of steps taken by the decoder in the environment)
- Polyak Averaging Coefficient: {0.95, 0.9}
- Number of parallel actors: 1
- Batch size: 128
- Replay buffer size: 1M

The best hyperparameters follow:

HRL-abs	Updates per Train Iter	Polyak Coefficient
CLEANHOUSE	1	0.95
FOURCORNER	8	0.9
HARVESTER	8	0.95
MAZE	1	0.95
STAIRCLIMBER	1	0.9
TOPOFF	1	0.9

HRL	Updates per Train Iter	Polyak Coefficient
CLEANHOUSE	1	0.9
FOURCORNER	1	0.95
HARVESTER	1	0.95
MAZE	8	0.9
STAIRCLIMBER	8	0.95
TOPOFF	8	0.95

L.4 Naïve

The naïve program synthesis baseline takes an initial token as input and outputs an entire program at each timestep to learn a recurrent policy guided by the rewards of these programs. We execute these

generated programs on 10 random environment start configurations in Karel to get the reward. We run PPO for 2M Karel environment timesteps. The policy network is comprised of one shared GRU layer, followed by two fully connected layers, for both the policy and value networks. For evaluation, we generate 64 programs from the learned policy, and choose the program with the maximum reward on 10 demonstrations. For each task, we perform a hyperparameter grid search over the following parameters, and report results from the run with the best averaged final reward over 5 seeds. We exponentially decay the entropy loss coefficient in PPO from the initial to final entropy coefficient to avoid local minima during the initial training steps.

- Learning Rate: 0.0005
- Batch Size (B): {64, 128, 256}
- initial entropy coefficient (E_i): {1.0, 0.1}
- final entropy coefficient: {0.01}
- Hidden Layer Size: 64

Hyperparameters that performed best for each task are listed below.

Naïve	B	E_i
WHILE	128	0.1
IFELSE+WHILE	256	1.0
2IF+IFELSE	256	0.1
WHILE+2IF+IFELSE	128	0.1

Naïve	B	E_i
CLEANHOUSE	128	0.1
FOURCORNER	128	1.0
HARVESTER	128	1.0
MAZE	256	1.0
STAIRCLIMBER	128	1.0
TOPOFF	128	1.0

L.5 VIPER

VIPER [12] builds a decision tree programmatic policy by imitating a given teacher policy. We use the best DRL policies as teachers instead of the DQN [124] teacher policy used in Bastani et al. [12]. We did this in order to give the teacher the best performance possible for maximum fairness in comparison against VIPER, as we empirically found the PPO policy to perform much better on our tasks than a DQN policy.

We perform a grid search over VIPER hyperparameters, listed below:

- Max depth of decision tree: {6, 12, 15}
- Max number of samples for tree policy: {100k, 200k, 400k}
- Sample reweighting: {True, False}

The best hyperparameters found for each task are listed below:

VIPER	Max Depth	Max Num Samples	Sample Reweighting
CLEANHOUSE	6	100k	False
FOURCORNER	12	100k	False
HARVESTER	12	400k	True
MAZE	12	100k	True
STAIRCLIMBER	12	400k	True
TOPOFF	15	100k	False

L.6 Program Embedding Space VAE Model

Encoder-Decoder Architecture. The encoder and decoder are both recurrent networks. The encoder structure consists of a PyTorch token embedding layer, then a recurrent GRU cell, and two linear layers that produce μ and $\log \sigma$ vectors to sample the program embedding.

The decoder consists of a recurrent GRU cell which takes in the embedding of the previous token generated and then a linear token output layer which models the log probabilities of all discrete tokens. Since we have access to DSL grammar during program synthesis, we utilize a syntax checker based on the Karel DSL grammar from Bunel et al. [17] at the output of the decoder to limit predictions to syntactically valid tokens. We restrict our decoder from predicting syntactically invalid programs by masking out tokens that make a program syntactically invalid at each timestep. This syntax checker is designed as a state machine that keeps track of a set of valid next tokens based on the current token, open code blocks (e.g. `while`, `if`, `ifelse`) in the given partial program, and the grammar rules of our DSL. Since we generate a program as a sequence of tokens, the syntax checker outputs at each timestep a mask M , where $M \in \{-\infty, 0\}^{\text{number of DSL tokens}}$, and

$$M_j = \begin{cases} -\infty & \text{if the } j\text{-th token is not valid in the current context} \\ 0 & \text{otherwise} \end{cases}$$

This mask is added to the output of the last layer of the decoder, just before the Softmax operation that normalizes the output to a probability over the tokens.

π Architecture. The program-embedding conditioned policy π consists of a GRU layer that operates on the inputs and three MLP layers that output the log probability of environment actions. Specifically, it takes a latent program vector, current environment state, and previous action as input and outputs the predicted environment action for each timestep.

To evaluate how close the predicted neural execution traces are to the execution traces of the ground-truth programs, we consider the following metrics:

- Action token accuracy: the percentage of matching actions in the predicted execution traces and the ground-truth execution traces.
- Action sequence accuracy: the percentage of matching action sequences in the predicted execution traces and the ground-truth execution traces. It requires that a predicted execution trace entirely matches the ground-truth execution trace.

After convergence, our model achieves an action token accuracy of 96.5% and an action sequence accuracy of 91.3%.

Training. The reinforcement learning algorithm used for the program behavior reconstruction \mathcal{L}^R is REINFORCE [64].

When training LEAPS with all losses, we first train with the Program Reconstruction (\mathcal{L}^P) and Latent Behavior Reconstruction (\mathcal{L}^L) losses, essentially setting $\lambda_1 = \lambda_3 = 1$ and $\lambda_2 = 0$ of our full objective, reproduced below:

$$\min_{\theta, \phi, \pi} \lambda_1 \mathcal{L}_{\theta, \phi}^P(\rho) + \lambda_2 \mathcal{L}_{\theta, \phi}^R(\rho) + \lambda_3 \mathcal{L}_{\pi}^L(\rho, \pi), \tag{6}$$

Once this model is trained for one epoch, we then train exclusively with the Program Behavior Reconstruction loss (\mathcal{L}^R), setting $\lambda_2 = 1$ and $\lambda_1 = \lambda_3 = 0$, with equal number of updates. These two update steps are repeated alternatively till convergence is achieved. This is done to avoid potential issues of updating with supervised and reinforcement learning gradients at the same time. We did not attempt to train these 3 losses jointly.

All other shared hyperparameters and training details are listed below:

- β : 0.1
- Optimizer: Adam (All optimizers)
- Supervised Learning Rate: 0.001
- RL Learning Rate: 0.0005

- Batch Size: 256
- Hidden Layer Size: 256
- Latent Embedding Size: 256
- Nonlinearity: $Tanh()$

L.7 Cross-Entropy Method (CEM)

CEM search works as follows: we sample an initial latent program vector from the initial distribution D_I , and generate population of latent program vectors from a $\mathcal{N}(0, \sigma I_d)$ distribution, where I_d is the identity matrix of dimension d . The samples are added to the initial latent program vector to obtain the population of latent program vectors which are decoded into programs to obtain their rewards. The population is then sorted based on rewards obtained, and a set of ‘elites’ with the highest reward are reduced using weighted mean to one latent program vector for the next iteration of sampling. This process repeats for all CEM iterations.

We include the following sets of hyperparameters when searching over the program embedding space to maximize R_{mat} to reproduce ground-truth program behavior or to maximize R_{mat} in the Karel task MDP.

- Population Size (S): {8, 16, 32, 64}
- μ : {0.0}
- σ : {0.1, 0.25, 0.5}
- % of population elites (this refers to the percent of the population considered ‘elites’): {0.05, 0.1, 0.2}
- Exponential σ decay⁵: {True, False}
- Initial distribution D_I : $\{\mathcal{N}(1, \mathbf{0}), \mathcal{N}(0, I_d), \mathcal{N}(0, 0.1I_d)\}$

Since a comprehensive grid search over the hyperparameter space would be too computationally expensive, we choose parameters heuristically. We report results from the run with the best averaged reward over 5 seeds. Hyperparameters that performed best for each task are listed below.

Ground-Truth Program Reconstruction We include the following sets of hyperparameters when searching over the program embedding space to maximize R_{mat} to reproduce ground-truth program behavior. We allow the search to run for 1000 CEM iterations, counting the search as a success when it achieves 10 consecutive CEM iterations with matching the ground-truth program behaviors exactly in the environment across 10 random environment start configurations. We use same hyperparameter set to compare LEAPS-P, LEAPS-P+R, LEAPS-P+L, and LEAPS.

CEM	S	σ	# Elites	Exp Decay	D_I
WHILE	32	0.25	0.1	False	$\mathcal{N}(0, 0.1I_d)$
IFELSE+WHILE	32	0.25	0.1	True	$\mathcal{N}(0, 0.1I_d)$
2IF+IFELSE	16	0.25	0.2	True	$\mathcal{N}(0, 0.1I_d)$
WHILE+2IF+IFELSE	32	0.25	0.2	False	$\mathcal{N}(0, 0.1I_d)$

MDP Task Performance We include the following sets of hyperparameters when searching over the LEAPS program embedding space to maximize rewards in the MDP. We allow the search to run for 1000 CEM iterations, counting the search as a success when it achieves 10 consecutive CEM iterations of maximizing environment reward (solving the task) across 10 random environment start configurations.

⁵Over the first 500 epochs, we exponentially decay σ to 0.1, and then we keep it at 0.1 for the rest of the epochs if True.

CEM	S	σ	# Elites	Exp Decay	D_I
CLEANHOUSE	32	0.25	0.05	True	$\mathcal{N}(1, \mathbf{0})$
FOURCORNER	64	0.5	0.2	False	$\mathcal{N}(0, 0.1I_d)$
HARVESTER	32	0.5	0.1	True	$\mathcal{N}(0, I_d)$
MAZE	16	0.1	0.1	False	$\mathcal{N}(1, \mathbf{0})$
STAIRCLIMBER	32	0.25	0.05	True	$\mathcal{N}(0, 0.1I_d)$
TOPOFF	64	0.25	0.05	False	$\mathcal{N}(0, 0.1I_d)$

L.8 Random Search LEAPS Ablation

The random search LEAPS ablations (LEAPS-rand-8 and LEAPS-rand-64) replace the CEM search method for latent program synthesis with a simple random search method. Both use the full LEAPS model trained with all learning objectives. We sample an initial vector from an initial distribution D_I and add it to either 8 or 64 latent vector samples from a $\mathcal{N}(0, \sigma I_d)$ distribution. We then decode those vectors into programs and evaluate their rewards, and then report the rewards of the best-performing latent program from that population.

As such, the only parameters that we require are the initial sampling distribution and σ . We perform a grid search over the following for both LEAPS-rand-8 and LEAPS-rand-64.

- σ : {0.1, 0.25, 0.5}
- Initial distribution D_I : $\{\mathcal{N}(0, I_d), \mathcal{N}(0, 0.1I_d)\}$

Ground-Truth Program Reconstruction We report hyperparameters below for both random search methods on program reconstruction tasks.

LEAPS-rand-8	σ	D_I
WHILE	0.1	$\mathcal{N}(0, 0.1I_d)$
IFELSE+WHILE	0.5	$\mathcal{N}(0, 0.1I_d)$
2IF+IFELSE	0.5	$\mathcal{N}(0, 0.1I_d)$
WHILE+2IF+IFELSE	0.5	$\mathcal{N}(0, 0.1I_d)$
LEAPS-rand-64	σ	D_I
WHILE	0.5	$\mathcal{N}(0, 0.1I_d)$
IFELSE+WHILE	0.5	$\mathcal{N}(0, 0.1I_d)$
2IF+IFELSE	0.5	$\mathcal{N}(0, 0.1I_d)$
WHILE+2IF+IFELSE	0.5	$\mathcal{N}(0, 0.1I_d)$

MDP Task Performance We report hyperparameters below for both random search methods on Karel tasks.

LEAPS-rand-8	σ	D_I
CLEANHOUSE	0.5	$\mathcal{N}(0, 0.1I_d)$
FOURCORNER	0.5	$\mathcal{N}(0, 0.1I_d)$
HARVESTER	0.5	$\mathcal{N}(0, 0.1I_d)$
MAZE	0.25	$\mathcal{N}(0, 0.1I_d)$
STAIRCLIMBER	0.5	$\mathcal{N}(0, I_d)$
TOPOFF	0.25	$\mathcal{N}(0, 0.1I_d)$

LEAPS-rand-64	σ	D_I
CLEANHOUSE	0.5	$\mathcal{N}(0, 0.1I_d)$
FOURCORNER	0.25	$\mathcal{N}(0, 0.1I_d)$
HARVESTER	0.5	$\mathcal{N}(0, 0.1I_d)$
MAZE	0.1	$\mathcal{N}(0, 0.1I_d)$
STAIRCLIMBER	0.25	$\mathcal{N}(0, 0.1I_d)$
TOPOFF	0.5	$\mathcal{N}(0, 0.1I_d)$

M Computational Resources

For our experiments, we used both internal and cloud provider machines. Our internal machines are:

- M1: 40-vCPU Intel Xeon with 4 GTX Titan Xp GPUs
- M2: 72-vCPU Intel Xeon with 4 RTX 2080 Ti GPUs

The cloud instances that we used are either 128-thread AMD Epyc or 96-thread Intel Xeon based cloud instances with 4-8 NVIDIA Tesla T4 GPUs. Experiments were run in parallel across many CPUs whenever possible, thus requiring the high vCPU count machines.

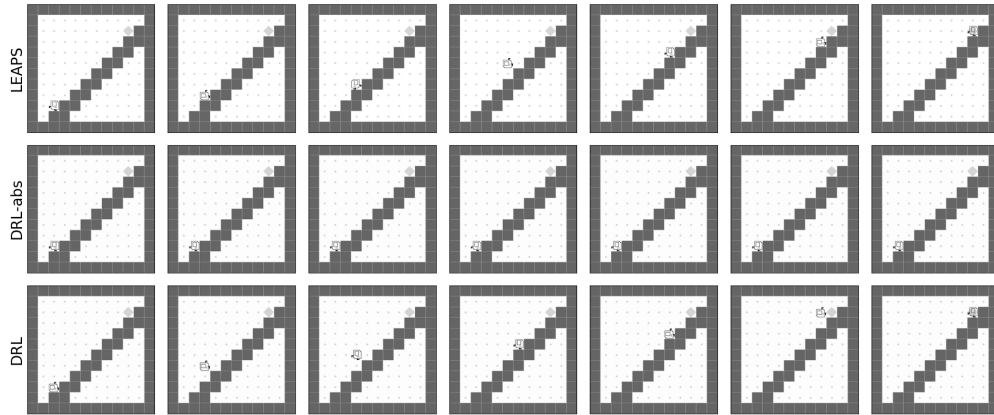
The experiment costs (GPU memory/time) are as follows:

Learning Program Embedding Stage:

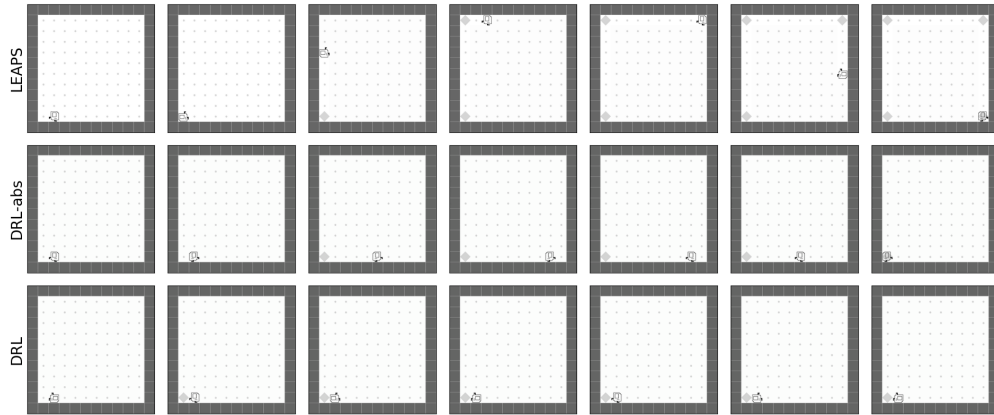
- LEAPS-P: 4.2GB/13hrs on either M1 or M2
- LEAPS-P+R: 4.2GB/44-54hrs on M2
- LEAPS-P+L: 8.7GB/26hrs on either M1 or M2
- LEAPS: 8.8GB/104hrs on M1, 8.8GB/58hrs on M2

Policy Learning Stage:

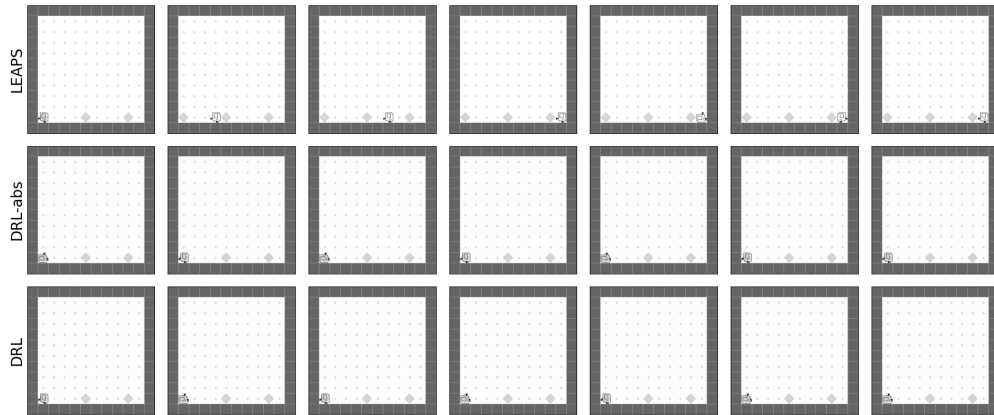
- CEM search: 0.8GB/4-10min (depends on the CEM population size and the number of iterations until convergence)
- DRL/DRL-abs/DRL-abs-t: 0.7-2GB/1hr per run with parallelization across 10 processes
- HRL/HRL-abs: 1-2GB/2.5hrs per run
- VIPER: 0.7GB/20-30 minutes (excluding the time for learning its teacher policy)



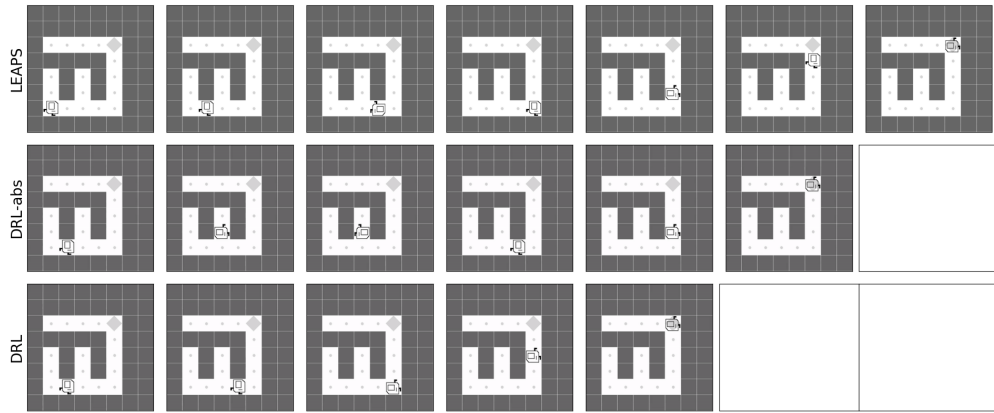
(a) STAIRCLIMBER: LEAPS and DRL are able to climb the stairs, DRL-abs is unable to do so.



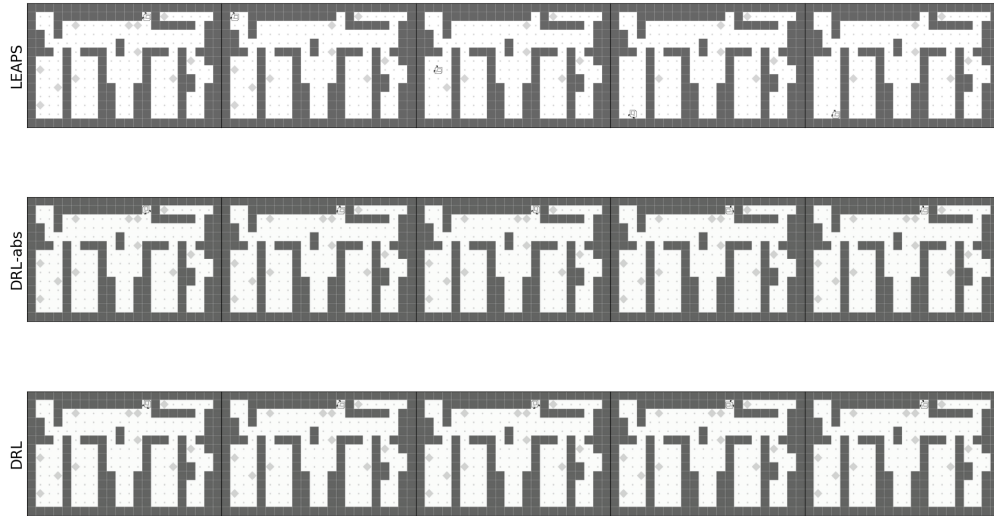
(b) FOURCORNER: In this example, LEAPS generates a program which is able to completely solve the task. Both DRL methods learn to only place one single marker in the left bottom corner.



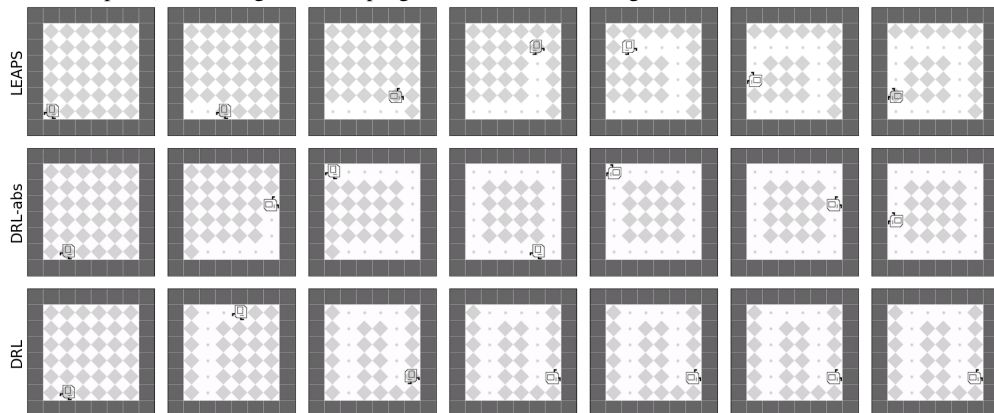
(c) TOPOFF: Here, LEAPS generates a program that solves the task by “topping off” each marker. Both DRL methods only learn to top off the initial marker.



(d) MAZE: All three methods are able to solve the task.



(e) CLEANHOUSE: While both DRL methods learn no meaningful behaviors (generally just spinning around in place), LEAPS generates a program that is able to navigate to and clean the leftmost room.



(f) HARVESTER: All three methods make partial progress on HARVESTER.

Figure 16: **Karel Rollout Visualizations.** Example rollouts for LEAPS, DRL-abs, and DRL for each task.